https://doi.org/10.5194/egusphere-2025-2021
Preprint. Discussion started: 26 May 2025

Qualification of an online device for the measurement of the oxidative potential of atmospheric particulate matter

Albane Barbero[1], Guilhem Freche[1], Luc Piard[1], Lucile Richard[1], Takoua Mhadhbi[1], Anouk Marsal[1], Stephan Houdier[1], Julie Camman[1,2], Mathilde Brezins[1,2], Benjamin Golly[3], Jean-Luc Jaffrezo[1], Gaëlle Uzu[1]

[1]Univ. Grenoble Alpes, CNRS, INRAE, IRD, Grenoble INP*, IGE, 38000 Grenoble, France*Institute of Engineering and Management Univ. Grenoble Alpes
[2]Aix Marseille Univ., CNRS, LCE, UMR 7376, 13331 Marseille, France
[3]Univ. Savoie Mont Blanc, CNRS, LOCIE (UMR 5271), 73376, Le Bourget-du-Lac, France

Correspondence to: Albane Barbero (albane.barbero@univ-grenoble-alpes.fr)

Abstract. Particulate Matter (PM) and gaseous pollutants can carry or induce the production of Reactive Oxygen Species (ROS) in the lung environment, causing oxidative stress, a key factor in the development of cardiovascular and pulmonary outcomes. Over the past decade, numerous techniques have been implemented to assess the Oxidative Potential (OP) of aerosols, i.e., their ability to oxidise the lung environment as an initial proxy of subsequent biological processes. Offline measurements from filters collected from air samplers are widely assessed but are probably underestimating PM redox activity due to the short lifetime of several ROS and/or the loss of the most volatile compounds on filters in a non-proportional and unsystematic way. This study introduces a new device, called *ROS-Online*, allowing the automatic and near real time measurement of two complementary OP assays, OP Ascorbic Acid (OP^{AA}) and OP Dithiothreitol (OP^{DTT}), sensitive to ambient PMs at mass concentrations about $[PM_{10}] \sim 20$ µg.m^{-3}. The *ROS-Online* device is designed to reproduce the exposure and interaction of airborne particles with the respiratory system. *ROS-Online* consists of three main modules: i) an air sampling module using a BioSampler® to collect airborne PM, ii) a distribution module that transports samples and reagents to iii) a measurement module that relies on spectrophotometric methods to monitor chemical reactions in real time. Its operation is based on established OP^{AA} and OP^{DTT} protocols, ensuring comparability with existing offline OP measurement methods. Compact and transportable (75 × 65 × 170 cm, 85 kg), *ROS-Online* is designed for deployment in air quality monitoring stations and allows for autonomous operation over two weeks. With a high particle collection efficiency (> 90 % by mass for PM_1 and $PM_{2.5}$) and greater sensitivity than offline methods, it provides accurate and reliable results across a wide range of aerosol concentrations, from urban backgrounds to highly polluted environments. The qualification of the device demonstrated an excellent correlation with offline methods for both OP^{AA} and OP^{DTT} measurements ($r > 0.96$), over positive controls, confirming the reliability and specificity of *ROS-Online* for continuous atmospheric aerosol OP monitoring. *ROS-Online* was deployed in the field, in an urban background site, where OP^{AA} of ambient air was measured for 15 continuous days and OP^{DTT} for 6 continuous days. Results showed a good correlation with ozone (O_3) signal ($R^2 = 0.74$), underlying the importance of considering pollutants' interaction in OP measurements, as laboratory experiment showed no OP response when introducing O_3 alone into the instrument. These preliminary results mark an important step towards establishing *ROS-Online* as a viable and effective tool for OP assessment in future research and monitoring endeavours.

https://doi.org/10.5194/egusphere-2025-2021
Preprint. Discussion started: 26 May 2025

1 Introduction

Air pollution has emerged as a critical public health issue and its exposure is considered to be the second most important risk factor for the total death rate for all sexes and ages in 2021 (State of Global Air Report 2024 | State of Global Air, 2024). An estimation was made of 8.1 million premature deaths worldwide in 2021, attributed to poor outdoor and household air quality due in large part to the significant contribution of particulate matter (PM) (WHO, 2023). This finding is drawn from cross-sectional studies based on mass concentrations of particulate matter (PM) in ambient air combined with health and mortality data. A significant number of epidemiological studies have linked some cardio-respiratory diseases and cancers, such as heart disease, stroke, diabetes, lung cancer, and chronic obstructive pulmonary disease to particulate matter exposure (Manigrasso et al., 2020; Manisalidis et al., 2020; Qu et al., 2017; Turner et al., 2020). While the complete mechanisms are not yet fully understood, studies point out that PM is responsible for generating oxidants *in vivo* and inducing inflammation, thereby leading to cellular damage (Møller et al., 2014, 2020). More specifically, these mechanisms are driven by oxidative stress and involve reactive oxygen species (ROS) carried or induced by PM (Campbell et al., 2019; Delfino et al., 2013; Strak et al., 2012) but also by certain trace gases (Dovrou et al., 2021a). Such mechanisms and rates of ROS production rely on the composition of the aerosol such as the presence of oxidised polyaromatics hydrocarbons (OPAH), organic peroxides (ROOR) or transition metals. Air quality monitoring policies are currently based on the measurement of PM total mass, but several studies invite to consider other parameters in future regulations since other physico-chemical parameters, among which, chemistry, size distribution, surface area, etc., broadly influence PM toxicity (Park et al., 2018; Song et al., 2021; Wittmaack, 2007). During the last decade, atmospheric scientists have been developing Oxidative Potential (OP) as a metric accounting for the redox and catalytic properties of PM (Calas et al., 2017; Cho et al., 2005). Recent studies demonstrated that at least in Europe, the OP of PM is driven by anthropogenic sources whereas the PM mass is mainly controlled by secondary inorganic components and crustal material, highlighting a different vision of the sources' impacts when using PM mass or PM OP (Daellenbach et al., 2020; Weber et al., 2021). Daellenbach et al. (2020) and Leni et al. (2020) also showed that the associations between pro-inflammatory lung biomarkers and $PM_{2.5}$ were higher for PM samples with the highest OP levels. Those findings strongly promote the health relevance of the OP metric. The new directive 2024/2881/CE was adopted on Nov 20th 2024 for the modification of the Directive 2008/50/EC on air quality in Europe**,** and specifically addresses the measurement of OP in airborne particulate matter. This new directive emphasizes on and recommends the measurement of OP as part of the broader assessment of air quality impacts on human health.

In the last 20 years, acellular methods have been developed to assess the redox activity of PM through various probes (Bates et al., 2015; Calas et al., 2018a; Rao et al., 2020a). Most of them rely on the depletion's quantification of a lung antioxidant, or surrogate, when in contact with PM. These traditional offline methods are widely used, and although they have a good recovery efficiency of the particulate matter, they involve bias in the estimation of OP. First, these methods probably underestimate PM redox activity due to the very short lifetime of some ROS (such as hydroxyl radical $^{\bullet}OH$) and/or the loss of the most volatile compounds (such as formaldehyde HCHO) in a non-proportional and unsystematic way (Jiang et al., 2019). Second, they do not allow near-real-time OP estimation, nor the OP analysis of soluble gases (Carlino et al., 2023). To overcome such drawbacks of offline methods, semi-

https://doi.org/10.5194/egusphere-2025-2021
Preprint. Discussion started: 26 May 2025

continuous prototypes for the OP measurement of solubilised PM filter samples and automatic on-site devices have recently been developed.

Indeed, semi-automatic laboratory methods for ROS analysis were developed based on the well-known dithiothreitol (DTT), ascorbic acid (AA) and dichlorofluorescin (DCFH) tests (Fang et al., 2015a; King and Weber, 2013; Yu et al., 2020a). Fuller et al. (2014) have designed a portable and integrated DCFH technique, allowing the PM sampling and solubilisation before their subsequent analysis (Fuller et al., 2014). Ambient air measurements at a London urban site confirmed that this device was sensitive enough to measure ambient ROS in a European urban environment, and showed the relevance of such instrument into air quality measurement stations (Wragg et al., 2016). More recently, a prototype coupling two probes (OP^{AA} and OP^{DCFH}) assessed online OP using fluorescence methods (Campbell et al., 2019; Utinger et al., 2023). The sensitivity of this device was tested on several transition metals, biogenic and anthropic secondary organic aerosol, and a mix of them, concluding that the method allowed for OP measurement in polluted urban environments (Campbell et al., 2023). Nevertheless, to the best of our knowledge, none is currently qualified for long term automatic online measurements. In addition, the different OP assays being sensitive at varying levels to diverse ROS-generating compounds (Lin et al. 2022), using several assays is crucial to provide a wider picture of the redox processes at stake.

The *ROS-Online* device, a stand-alone prototype for near-real-time measurement of ambient air OP *via* two complementary assays, is currently under development at the Institute for Environmental Geosciences (IGE, Grenoble, France). The device integrates two independent measurement lines, allowing the simultaneous measurements of ascorbic acid OP (OP^{AA}) and dithiothreitol OP (OP^{DTT}). Both tests are known for their physiological, practical, and economic advantages, and are widely used in offline methods (Dominutti et al., 2025; Mudway et al., 2004; Perrone et al., 2019; Rao et al., 2020b). This device differs from others by assessing both OP^{AA} and OP^{DTT} from a unique atmospheric sample collected through a BioSampler® (SKC) for both soluble gases and particulate matter. The present paper first presents in section 2 the *ROS-Online* device and its main characteristics and operating principles. Section 3 is devoted to the sampler characterisation and *ROS-Online*'s response evaluation in a simulated polluted environment with controlled airflow conditions. Section 4 presents the calibration of the two OP assays of *ROS-Online*, including an intercomparison with offline measurements, the latter being routinely implemented at IGE (e.g., Calas et al., 2017b, 2018b; Dominutti et al., 2023, 2024; Weber et al., 2018). Section 5 presents atmospheric measurements using *ROS-Online* under real conditions at a traffic site.

https://doi.org/10.5194/egusphere-2025-2021
Preprint. Discussion started: 26 May 2025

2 The *ROS-Online* device

2.1 Description and main characteristics

ROS-Online simulates pulmonary exposure and interaction with ambient air, aiming to replicate the physiological processes of inhalation and respiratory surface contact. The device is patented (PCT PCT/EP2021/080824, number WO2022096675, 12.06.2022. Priority: FR 20 11431 ROS ONLINE). The operating and measurements principles rely on the existing offline protocols for OP^{AA} and OP^{DTT}. This choice will allow to compare the overall body of data already available for offline OP measurements with that produced by *ROS-Online*. The prototype is described in Fig. 1 and consists of three main modules: i) the sampling module for the ambient air collection, ii) the distribution module, and, iii) the measurement module for chemical reaction monitoring. An additional computer is used for managing the device and all data processing steps using LabVIEW application.

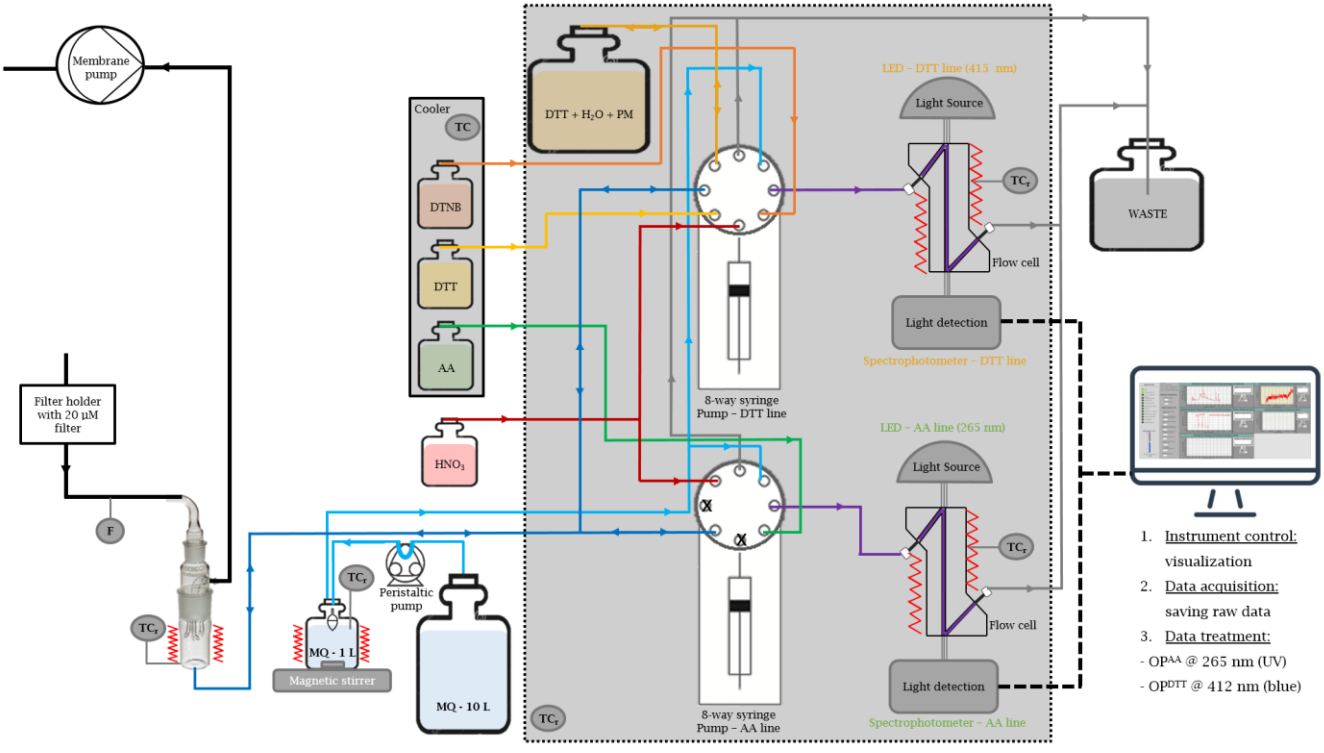

Figure 1. *ROS-Online* diagram

2.1.1 Offline method and adaptation to *ROS-Online*

The offline method originally adapted from Cho et al., 2005 and Li et al., 2009a is fully described in Calas et al., 2017; Weber et al., 2018, 2021. Briefly, PM extracts from atmospheric filters are introduced into two 96-well plates kept at physiological conditions (pH = 7.4, T = 37 °C) and are shaken for 60 s for DTT and for 10 s for AA, to insure homogeneity. The absorbance of the matrix is then read after 10 s or 3 s, for AA and DTT, respectively. AA and DTT are then respectively added in each plate to initiate their oxidation by PM induced ROS. Both measurements are run in parallel by different spectrophotometers to avoid different ageing of

https://doi.org/10.5194/egusphere-2025-2021
Preprint. Discussion started: 26 May 2025

the PM extraction. AA depletion is monitored continuously for 30 min by measuring the absorbance at λ = 265 nm using a plate reader spectrophotometer (TECAN, model M1000 Infinite), AA depletion rate being determined by linear regression. DTT depletion is indirectly quantified by titrating the remaining amount of DTT with dithionitrobenzoic acid (DTNB) at different reaction times (0, 15, and 30 min). The reaction produces a coloured compound (5-thio-2-nitrobenzoic acid or TNB) which absorbs at λ = 412 nm and the absorbance is measured using a spectrophotometer plate reader (TECAN, model M200 Infinite). Ascorbic acid and dithiothreitol depletions are monitored by recording the absorbance at 265 nm and 412 nm, respectively, using the Beer-Lambert law (Eq.1):

$$A = \varepsilon . L . c = log\left(\frac{I_0}{I}\right), \quad (1)$$

where A is the absorbance; ε is the molecular extinction coefficient [l.mol^{-1}.cm^{-1}]; L is the optical path, i.e., the wells' depth for the off-line method and the flow cell (FC) length [cm] for the *ROS-Online* device, I is the transmitted intensity of the solution; I_0 is the intensity at t = 0 min; and c is the followed antioxidant concentration (AA) or the concentration of its reaction product (TNB) in the flow cell [mol.l^{-1}]. Both AA and DTT consumption rates, ω, are calculated following Eq. 2:

$$\omega = -s\,\frac{\eta_0}{A_0}, \quad (2)$$

where s is the slope value of the linear regression of the measured absorbance over time [s^{-1}] ; A_0 is the absorbance at t = 0 min ; and η_0 is the initial quantity of reagent [mol] injected into the wells or the FC. Blanks for *ROS-Online* are measured by replacing the extracted PM solution with ultra-pure water (Type 1 Milli-Q® or MQ). In the offline methods, filter and field blanks are made to consider the possible quartz fibre fragments absorbance and / or the handling contamination. The oxidative potential (OP) of ambient air is expressed as the probe's (AA or DTT) consumption rate ω_{run} subtracted from the blank consumption rate ω_{blank} per sampled air volume following the method described in Fang et al., 2016a, 2015b. This metric, expressed in nmol.min^{-1}.m^{-3}, considers all the volumes involved in the experiment, following Eq. 3 for the *ROS-Online* device:

$$OP = \frac{\omega_{run} - \omega_{blank}}{V_s \cdot \frac{V_{FC}}{V_{BS}}}, \quad (3)$$

where V_s is the ambient air volume sampled by *ROS-Online*; V_{FC} the FC volume; and V_{BS} the final sampled volume, considering evaporation in the sampling device, i.e. a modified BioSampler® (U.S Patent No. 5,902,385).

For polluted environments such as European urban background sites, the sensitivity of the device allows one measurement of both OP^{AA} and OP^{DTT} assays on a 20 min atmospheric sampling period every 60 min. The output final data are expressed in nmol.min^{-1}.m^{-3}, the now well-established unit for OP normalized per m^3 (Dominutti et al., 2025). The global size of the device is 75 x 65 x 170 cm, in the format of a rack with wheels, weighing 85 kg. The electrical power needed is about 800 W and the rack can easily fit in an Air quality monitoring station. *ROS-Online* requires an environment with temperature between 15 and 30 °C. All parts of the device are controlled in temperature. It is easily movable and can be up and running in a couple of hours. Finally, the current autonomy is about two weeks for continuous measurements on both lines due to the consumption and storage of ultra-pure water required for the measurement.

https://doi.org/10.5194/egusphere-2025-2021
Preprint. Discussion started: 26 May 2025

2.1.2 Prototype features

Airborne PM and soluble gases are collected into a BioSampler® filled with 20 ml MQ water by pumping ambient air at a constant flow rate of ~ 10.5 l.min^{-1}. This airflow is monitored by using a Venturi flow meter. The BioSampler® nozzle section contains three tangential 0.630 mm nozzles that act as sonic orifices that maintains a pressure drop of ~ 0.5 atm or more across the sampler at normal atmospheric conditions (sonic flow) (BioSampler, 2024). Nebulisation of the water is generated *via* the nozzles during vacuuming ensuring optimal gas/liquid exchange and homogenisation of the solution. The BioSampler® is kept in a controlled chamber at a temperature of 37 °C. Evaporation may occur during the 20 min pumping period, due to temperature and pressure differences between ambient air and air in the device. Temperature and humidity sensors installed at the inlet and outlet of the unit allow to assess the actual water sample volume left at the end of each sampling period. The device requires fluids for air sampling, rinsing between each measurement, and to perform OP^{AA} and OP^{DTT} measurements following protocols described above. A 20 l Jerrycan (GDPE Nalgene®) of MQ water automatically feeds a heated glass tank (1 l) that delivers water for collection and reactions at physiological temperature. Tanks containing AA (185 µM), DTT (2.12 mM) and DTNB (2.12 mM) solutions are sheltered from the light and stored at T = 4 °C in a cooler. The rinsing solution (HNO_3 0.1 % in MQ water) is stored in 2 l tank. All fluids are distributed by two 8-channel syringe pumps (PUMP Cadent 6 48K Level 3 – Norgren) *via* PTFE tubing (1/16").

2.1.3 Spectrophotometric monitoring of the reaction

Each line of measurement has its own {light source + spectrophotometer} couple: {ILR-ZZ01-Z265-LS0xx-SC201 (Stanley) + MAYA 2000 Pro (Ocean Optics)} and {M415F3 (Thorlabs) + MAYA 2000 Pro (Ocean Optics)} for the AA and DTT assays respectively. For kinetic monitoring of the reaction, AA+PM and DTT+DTNB+PM mixtures are pushed respectively into two microfluidic Z-flow cells (100 mm PEEK - IDIL), equipped with pressure controllers to avoid bubble formation that could compromise the absorbance measurement.

2.1.4 Comparison with other online devices

Several automated and semi-automated prototypes characterising OP have been reported in the literature. Fang et al. (2015b) and Gao et al. (2017) adapted the widely used OP^{DTT} measurement, while Campbell et al. (2019) proposed a prototype based on AA chemistry following the design presented in Wragg et al. (2016). Eiguren-Fernandez et al. (2008) developed an online monitor which combined a liquid spot sampler and a chemical module optimized for online OP^{DTT} measurements. Finally, Yu et al. (2020b) set a multi-endpoint analyser including both OP^{AA} and OP^{DTT} assays. It should be noted that initial concentrations of reagents differ from one study to another as well as some of the experimental conditions. For example, the solubilisation medium used to solubilise airborne PM do not present the same chemical composition for each device (see discussion below). As shown in Table 1, comparison for both assays with other developed prototypes concludes to a much better background noise or blank for *ROS-Online*. The limit of detection (LOD) of *ROS-Online* was defined as $LOD = \omega_{blank-mean} + 3\,\sigma$, where σ is the standard deviation calculated over n measurements of pure MQ water blanks (Fang et al., 2015b; King and Weber, 2013). *ROS-Online* LODs for OP^{AA} and OP^{DTT}

https://doi.org/10.5194/egusphere-2025-2021
Preprint. Discussion started: 26 May 2025

assays in standard operation conditions were (0.58 ± 0.24) pmol.min^{-1} (n = 342 over a period 15 days) and (25.4 ± 4.0) pmol.min^{-1} (n = 118 over a period of 6 days), respectively. In comparison, LOD for IGE's offline methods were (6.70 ± 0.78) pmol.min^{-1} (OP^{AA} assay, n = 36) and (19.93 ± 3.01) pmol.min^{-1} (OP^{DTT} assay, n = 36). *ROS-Online* is about twice more sensitive in measuring OP^{AA} than the offline IGE method and exhibits an equivalent sensitivity than the OP^{DTT} assays in the already published online methods. As shown later, such a sensitivity allows OP measurements over 20 minutes in operating conditions for the European environments we studied. Calibration experiments with artificial solutions of PM redox components like $CuCl_2$ or phenantroquinone (PQN) (more information in Section 4.) show that *ROS-Online* exhibits linearity over a high dynamic range of concentrations for these species. This is possible because *ROS-Online* allows large antioxidants depletions, i.e., high value of s in Eq. 2, from few pmol.min^{-1} to thousands of pmol.min^{-1} or hundreds of pmol.min^{-1} for AA and DTT assays, respectively. This result let us assume that *ROS-Online* could be employed in very polluted environment (industrial sites, mining industry, smog cities etc.). The comparison with consumption rates (ω) achieved for calibrations in other studies (Table 1) highlights the influence of reactant concentrations on OP values. The signal to noise ratio (SNR) of *ROS-Online* is calculated for each assay following equation (4):

$$SNR = \sum_{t=0}^{t=2} \frac{I_t}{\sigma_I}, \quad (4)$$

where I_t is the intensity (arbitrary units) of the spectrophotometric measurement of the sample at different times: t = 0 – reference, only MQ water is introduced in the measuring cells; t = 1 – start, the sample is introduced in the FC and the intensity is monitored after 60 s of reaction; and t = 2 – end, the intensity read at the end of the reaction, i.e., at t = 10 min for AA and t = 15 min for DTT. σ_I is the standard deviation on the intensities over 6 days of atmospheric monitoring. The maximum SNRs measured for AA and DTT assays were (39 ± 2) and (23 ± 5), respectively. Therefore, *ROS-Online* presents good sensitivity and low limit of detection (LOD), allowing to accurately quantify small variations in OP^{AA} and OP^{DTT} responses in near-real-time measurements of atmospheric PM.

Table 1. Comparison for existing prototypes

	LOD_{AA} pmol.min^{-1}	LOD_{DTT} pmol.min^{-1}	$[AA]_0$ µM	$[CuCl_2]$ range µM	ω_{AA} nmol.min^{-1}	$[DTT]_0$ µM	[PQN] range µM	DTT depletion µmol.min^{-1}
Fang *et al.* 2015	-	0.31				10^3	0.14 – 0.35	(0.2 – 2) ×10^3
Eiguren-Fernandez *et al.* 2017	-	0.15				0.1	0.025 – 0.25	(0.25 – 2.3) × 10^{-3}
Gao *et al.* 2017	-	0.21				10^3	0.07 – 0.28	(0.2 – 1.3) × 10^3
Puthussery *et al.* 2020	-	0.24				10^3	0.04 – 0.20	0.2 – 1.6
Yu *et al.* 2020	197 × 10^{-6}	60 × 10^{-6}	2 × 10^4	0.2 – 1	(2.5 – 5.0) × 10^5	10^3	0.05 - 0.25	0.75 – 2.5
This study	(0.58 ± 0.24)	(25.4 ± 4.0)	185	0.005 – 0.050	0.015 – 0.041	212	0.05 – 0.150	0.052 – 0.099

3 *ROS-Online* response under semi-controlled environment

A laboratory test-bench was used to characterize the response of the *ROS-Online* to atmospheric components under semi-controlled operating conditions. This was performed on a bench from LOCIE (Building Energy Processes Laboratory) in University of Savoie-Mont Blanc, Chambery, France. These tests aimed at evaluating the ability of *ROS-Online* to capture PMs, by studying the collection

https://doi.org/10.5194/egusphere-2025-2021
Preprint. Discussion started: 26 May 2025

efficiency of the BioSampler® and will be compared to results obtained with the same device in recent studies (Bøifot et al., 2024; Lin et al., 2018; Mescioglu et al., 2021). Measurements with specific particles directed to the inlet of the instrument were achieved to evaluate the capability of *ROS-Online* to detect and measure ambient OP in near real atmospheric conditions. Fig. 2 shows a schematic representation of the experimental set-up made of stainless-steel pipes (internal diameter 72 mm). The carrier gas used is ambient air from the laboratory, pre-filtered by a HEPA (U15 -EN1822- with a MPPS, or most penetrating particle size, = 99,9995%) filter and the air flow (FI) is controlled by a variable speed fan allowing a flow rate from 5 $m^3.h^{-1}$ to 70 $m^3.h^{-1}$. The bench is also equipped with thermo-hygrometers measuring the temperature (TI) and relative humidity (RH) during experiments. Finally, the potential impact of oxidising gases on the *ROS-Online* response was also studied by injecting variable O_3 concentrations (in the 0-50 ppb range) directly at the sampling inlet of the *ROS-Online* system.

3.1 BioSampler® characterization of collection efficiency

A first characterization of PM collection efficiency is carried out with the BioSampler® only, by sequential opening of the three-way valve (Fig. 2 – ways (A) and (B)) during sampling times of 15 min. Particle size distribution and PM concentration within the bench are monitored using two devices: an optical PM counter (particles range between 0.3 µm and 20 µm - model 1.108, Grimm) and a portable scanning mobility particle sizer, NanoScan® SMPS (nanometric particles 10 nm to 300 nm - model 3910, TSI Inc.) equipped with a X-ray pre-neutralization step (model 3088, TSI Inc.) prior to the sample analyses (Fig. 2). An aerosol of liquid particles is generated using a nebulizing particle generator (model ATM220, Topas) supplied with dry and filtered air. A 1 $g.l^{-1}$ KCl solution was used to generate a saline aerosol with normalized size distribution of particles. Relative humidity and temperatures were 40 % and 25 °C, respectively, the atomisation rate was set at 1 $ml.min^{-1}$ (or 6.0 x 10^{-5} $m^3.h^{-1}$), and the bench air-flow was 20 $m^3.h^{-1}$.

https://doi.org/10.5194/egusphere-2025-2021
Preprint. Discussion started: 26 May 2025

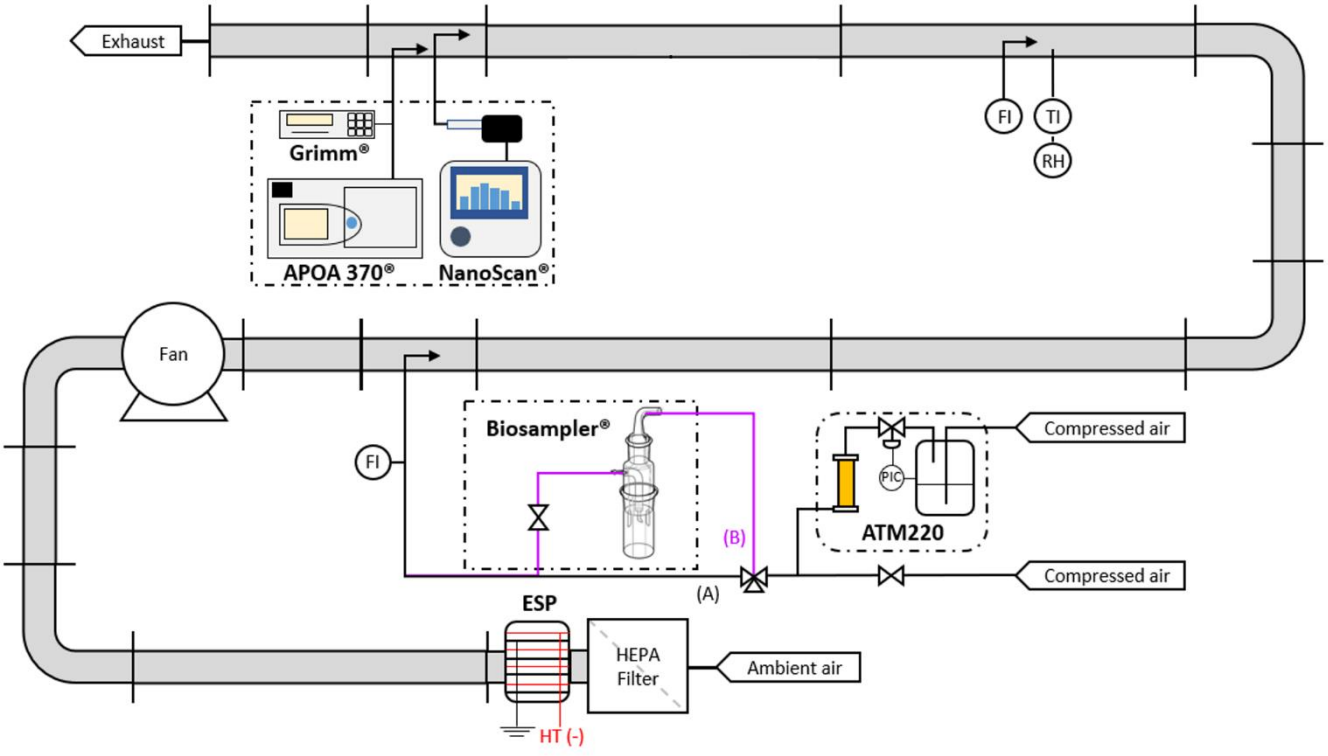

Figure 2. Schematic diagram of the experimental bench at LOCIE laboratory: the figure shows the set-up for the BioSampler® collection efficiency experiment.

This methodology has been commonly used at LOCIE laboratory and described in detail in Chen et al. (2020). Shortly, the measurement of PM concentration for each i-th class of diameter (n = 3 replicates) was performed between 20 nm and 5 µm. Firstly, a bypass of the BioSampler® (way-A) was used to determine the initial injected PM concentration which was subsequently measured after the air flow passed through the BioSampler® following the B-way (pink). The difference of particle number measured by these two ways allowed to calculate the single-pass fractional collection efficiency $\eta(d_p)$ for each class of diameter, which is defined by:

$$\eta(d_p) = \left(1 - \frac{N_{B,i}}{N_{A,i}}\right).100, \quad (5)$$

where $N_{A,i}$ and $N_{B,i}$ are the number of particles (cm^{-3}) measured for each class of diameter through A- and B-ways, respectively. The fractional collection efficiency at different flow rates calculated using Eq. 5 are reported in Fig. 3. It shows U-shaped curves which are typically reported in literature for this type of bioaerosol sampler (Bøifot et al., 2024; Guo et al., 2024; Su and Vincent, 2004).

https://doi.org/10.5194/egusphere-2025-2021
Preprint. Discussion started: 26 May 2025

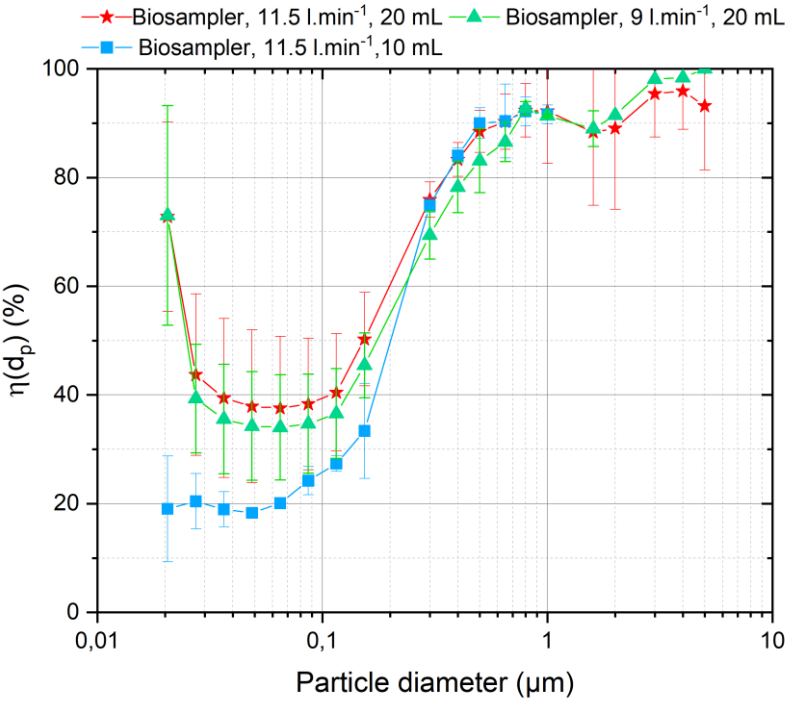

Figure 3. Fractional number efficiency of BioSampler® at several airflow rates.

In this study, efficiencies of BioSampler® were tested at sampling flow rates of 9 l.min^{-1} and 11.5 l.min^{-1}. At 11.5 l.min^{-1}, the BioSampler® was filled with 10 or 20 ml of MQ water to evaluate the influence of evaporation. Similar results were obtained for both flow rates, with fractional collection efficiencies $\eta(d_p)$ in the range (34 ± 9.7) % – (37.6 ± 14.6) % at 65 nm and in the range (88.5 ± 3.5) % – (100 ± 7.0) % above 500 nm. The low fractional collection efficiencies ($\eta(d_p) \sim 40$ %) for particles in the range (50 – 80) nm are similar to the results reported by Li et al. (2018). In the size range of 0.5 µm to 5 µm, the $\eta(d_p)$ above 90 % are also consistent with the literature values (Bøifot et al., 2024; Guo et al., 2024; Su and Vincent, 2004). $PM_{2.5}$ collection efficiencies by mass, recalculated from number distributions, were close to 82 % to 85 %. Indeed, KCl atomisation produces few large particles, therefore the total mass is only 70 % carried by particles larger than 300 nm. In atmospheric aerosol, on the other hand, large particles (> 300 nm) account for most of the mass (> 90 %). Therefore, the lower collection efficiency we measured for particles < 0.3 µm will only produce a limited loss of total mass in the 10 nm – 10 µm range.

As shown in Figure 3 for experiments with different sampling volumes, the loss of sampling liquid through evaporation also reduces the collection efficiency, especially for nanometric particles (< 100 nm). This is likely because of a lower aerosolization of the collection liquid when the distance between the inlet nozzles and the liquid surface increases. These results suggest that the collection efficiency for nanometric particles may significantly decline over prolonged sampling durations, thereby supporting the choice to fill the BioSampler with 20 ml of ultrapure (MQ) water in subsequent measurements.

https://doi.org/10.5194/egusphere-2025-2021
Preprint. Discussion started: 26 May 2025

3.2 Atmospheric OP with semi controlled PM generation

Four experiments were conducted with artificial solutions of $CuCl_2$ and Naphthoquinone (NQ), both being major redox components of PM (Ayres et al., 2008; Charrier and Anastasio, 2012; Kumagai et al., 2002) to evaluate the *ROS-Online* response and to highlight the difference in reactivity of both probes. Experimental conditions are resumed in Table 2. *ROS-Online* collected over 20 min at 0.6 $m^3.h^{-1}$ (~ 10.5 $l.min^{-1}$) inside the main air flow at 20 $m^3.h^{-1}$. An isokinetic calculation was performed to adjust the same velocity in the gas stream and in the *ROS-Online* sampling line. Laminar flow conditions were ensured by the distances between the disturbance zones and the tapping points, i.e., 3 times the pipe diameter upstream and 10 times the pipe diameter downstream. The size distribution of the particles generated during the four experiments is presented in Fig. S1 of the supplementary materials. Experiments 1 and 2 were conducted with a 47 nM $CuCl_2$ solution atomised in the experimental bench at two different rates, 1 and 0.5 $ml.min^{-1}$, respectively, in order to achieve different concentration levels of PMs. Indeed, between experiment 1 and 2, PM concentrations changes from (64 ± 10) to (34 ± 5) $\mu g.m^{-3}$ for $PM_{2.5}$ and from (59 ± 9) to (30 ± 5) $\mu g.m^{-3}$ for PM_1. Experiments 3 and 4 were conducted using 1 mM and 8 mM solutions of NQ respectively, leading to PMs concentration levels of (215 ± 18) to (364 ± 18) $\mu g.m^{-3}$ for $PM_{2.5}$ and (179 ± 6) to (323 ± 13) $\mu g.m^{-3}$ for PM_1. Regardless of the concentration of the solutions or the atomisation rate, the nebulized particle generator produces a majority of PM_1, with an average of (88 ± 4) % of the particles by mass having a diameter of 1 µm or less.

Table 2. Experimental conditions

Experiment number	Compound	Concentration	Atomisation rate $ml.min^{-1}$	Bench Airflow $m^3.h^{-1}$	T °C	RH %
1	$CuCl_2$	47 µM	1	20	18.0	24.0
2	$CuCl_2$	47 µM	0.5	20	18.0	24.0
3	NQ	1 µM	0.5	20	18.0	24.0
4	NQ	8 µM	0.5	20	18.0	24.0

Figure 4 shows the results for the different experiments on both assays of *ROS-Online*.

https://doi.org/10.5194/egusphere-2025-2021
Preprint. Discussion started: 26 May 2025

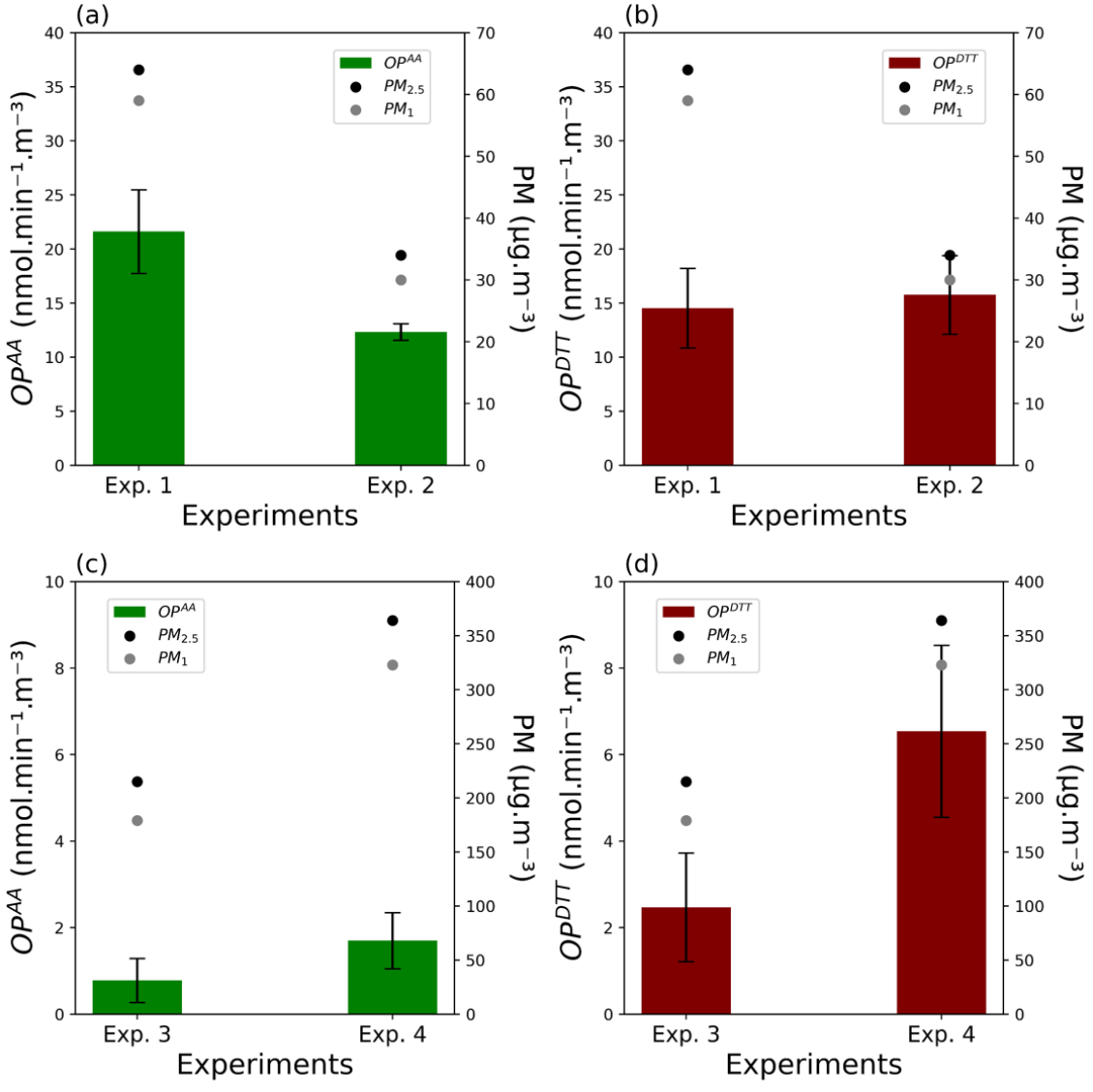

Figure 4. (a), (c) OP^{AA} and (b), (d) OP^{DTT} results obtained during the four experiments carried out in the experimental bench. Dots represent the average $PM_{2.5}$ (black) and PM_1 (grey) mass concentrations (µg.m^{-3}) in the main flow, bars represent the OP ± 1σ (nmol.min^{-1}.m^{-3}) of AA (green) and DTT assays (brown).

As shown in Fig. 4 (a) and (b) for $CuCl_2$ experiments 1 and 2, OP^{AA} confirmed its high metal-sensitivity (Calas et al., 2018a; Fang et al., 2016b; Godri et al., 2011) with OP values of (21.6 ± 3.9) and (12.3 ± 0.8) nmol.min^{-1}.m^{-3}. This result is consistent with the common observation that ascorbic acid is especially sensitive to transition metals which are known to catalyse the oxidation of AA through Fenton-type radical reactions (Bates et al. 2019 ; Fang et al. 2016 ; Bresgen et Eckl 2015 ; Pietrogrande et al. 2022). OP^{DTT} results show significant but less heterogeneous values, (14.5 ± 3.7) and (15.8 ± 3.6) nmol.min^{-1}.m^{-3}, respectively, as already evidenced in the literature (Charrier and Anastasio, 2012; Lin and Yu, 2011; Pietrogrande et al., 2022a).

https://doi.org/10.5194/egusphere-2025-2021
Preprint. Discussion started: 26 May 2025

$PM_{2.5}$ and PM_1 concentrations in the bench are divided by a factor of two between experiments 1 and 2. Interestingly, rather different ratios of 1.8 and 0.9 were observed for OP^{AA} and OP^{DTT} between the 2 experiments. Thus, the response of the DTT assay to copper particles seems to reach a maximum, regardless of their mass concentration. However, it remains unclear whether this represents an absolute maximum for OP^{DTT} or a local plateau that could rise further if concentrations still increases. This observation could be explained by the intricate two-stage kinetics of the reaction between DTT and oxygen in the presence of copper which, as already observed for lead (Uzu et al., 2011), involves the formation of a [DTT-Cu] complex (Kachur et al., 1997) and thus limits the redox reactivity between the two compounds.

Regarding NQ experiments 3 and 4 (Fig. 4 (c) and (d)), $PM_{2.5}$ and PM_1 concentrations in the bench are not proportional to the concentration of the solutions used for nebulization. Indeed, while an 8 times more concentrated solution is used for experiment 4, the ratio of PMs concentrations between the two experiments does not exceed 1.7 and 1.8 for $PM_{2.5}$ and PM_1, respectively. Considering OP values, OP^{AA} appears to be less sensitive to NQ than OP^{DTT} in these conditions, with OP^{AA} values of (0.8 ± 0.5) (Exp. 3) and (1.7 ± 0.7) (Exp. 4), and OP^{DTT} values of (2.5 ± 1.3) (Exp. 3) and (6.5 ± 2.0) $nmol.min^{-1}.m^{-3}$ (Exp. 4). This has already been observed by Pietrogrande et al. (2022). Indeed, DTT is reactive to both organic and inorganic compounds and its high reactivity towards quinones has been highlighted many times (Calas et al. 2018; Jiang et al. 2020; Yang et al. 2014). However, both assays show an increase in OP values with PM concentrations, even though this increase is not proportional with ratios of 2.2 and 2.6 for OP^{AA} and OP^{DTT}, respectively. A non-proportional increase in PMs concentrations could be explained by many parameters such as the non-controlled NQ aerosol generation with the nebulized particle generator as organic aerosols like naphthoquinones might interact with stainless steel surfaces under varying conditions (Sherif and Park, 2006; Walker et al., 2022).

3.2.1 ROS-Online interference with ozone

Dovrou et al. (2021) highlighted the key role of ozone in the formation of ROS like H_2O_2, $^{\bullet}OH$, $^{\bullet}O_2^-$, or $H^{\bullet}O_2$. Additionally, Stevanovic et al. (2017) have demonstrated the presence of ROS in both gaseous and particulate phases of vehicular emissions. To test for this hypothesis, *ROS-Online* sensitivity to an oxidant gas such as O_3 was explored in controlled conditions. In these experiments, O_3 delivered by a 2B Tech O_3 generator was introduced into the air stream sampled by *ROS-Online*, and a Thermo Scientific Model 49i O_3 analyser was used to measure O_3 levels at the exhaust of *ROS-Online*. This set-up allowed 100 % of the O_3 introduced into the *ROS-Online*'s airflow to be collected during sampling. O_3 was introduced at concentrations ranging from 0 to 50 ppbv resulting in quite uniform AA depletions (Fig. S2 of the supplementary) with mean and median values of (4.2 ± 1.1) and 4.0 $pmol.min^{-1}$, respectively. Therefore, *ROS-Online*'s response seems not be correlated influenced by the ozone concentration present in the atmosphere. Indeed, the oxidative potential of O_3 is not effectively captured via AA depletion in *ROS-Online*, potentially because: 1) ozone adsorbs or reacts with surfaces (e.g. pipes) before entering the sampler, or 2) ozone is not very soluble in water and/or the contact time between water and air is insufficient, so it cannot be trapped. In atmospheric conditions, it tends to adsorb / react with surfaces or airborne particles before it can dissolve in a liquid-phase assay (Bates et al., 2019; Bellini and De Tullio, 2019; Chang et al., 2021; Charrier and Anastasio, 2012).

https://doi.org/10.5194/egusphere-2025-2021
Preprint. Discussion started: 26 May 2025

4 *ROS-Online* linearity assessment with positive controls and exposed samples

$CuCl_2$ ([5– 50] nM) and PQN ([5 – 150] nM) standard solutions were selected to assess the OP^{AA} and OP^{DTT} sensitivities, respectively, of the system. Concentrations ranges for Cu(II) and PQN were chosen to be representative of concentration levels measured in European cities (Delgado-Saborit et al., 2013; Denier van der Gon et al., 2013; Liu et al., 2024; Yang et al., 2018). Extract solutions from two real PM samples, collected in the peri-urban area of Grenoble and at a traffic site in Bern (Switzerland) were also analysed, for OP^{DTT} and OP^{AA}, respectively. Both samples were collected on pre-baked quartz filters (Pall, Tissuquartz) with a high-volume sampler (Digitel, DA80, 30 $m^3.h^{-1}$) equipped with a PM_{10} inlet. The filters were extracted in MQ water in a multi-tube vortex at 37 °C. In order to avoid any clogging of the prototype lines by remaining fragments from the quartz filters, syringe filters (Sartorius, 0.2 µm) were used to filter the extracted samples. Calibration solutions in the [0.05 – 1.86] µg $PM.ml^{-1}$ range (equivalent to [5 – 180] $\mu g.m^{-3}$ atmospheric PM concentrations (Borlaza et al., 2022)) for the Grenoble filter and in the [0.05 – 1.05] µg $PM.ml^{-1}$ range ([5 – 100] $\mu g.m^{-3}$ equiv. PM) for the Bern sample were prepared. Each standard solution was analysed for OP in triplicate and the three replicates were used to calculate the standard deviations for the online method. Blanks containing only MQ water were analysed prior the standard solutions and their values are reported in Table 5. Figure 5 (a)-(d) shows *ROS-Online* response (corrected for the blanks) over the $CuCl_2$ and PQN ranges for both AA and DTT assays. Except for PQN in the AA assay (Fig. 5(c)), the *ROS-Online* response is shown to be linear with determination coefficients in the range $0.957 < R^2 < 0.983$.

https://doi.org/10.5194/egusphere-2025-2021
Preprint. Discussion started: 26 May 2025

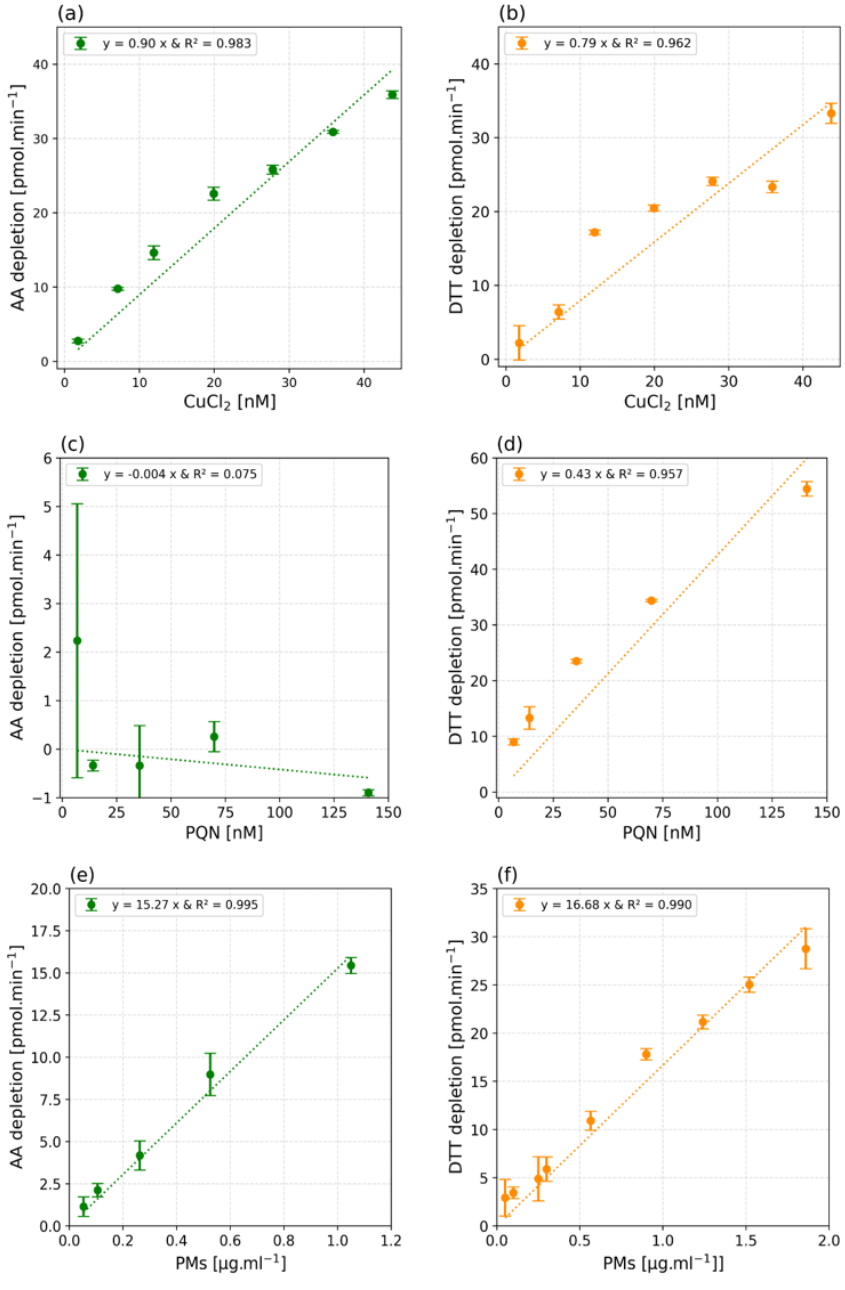

Figure 5. Green dots represent the ascorbic acid consumption rate, i.e., depletion, in [pmol.min^{-1}] as a function of $CuCl_2$ (a) and PQN (c) concentrations in [nM]. The orange dots represent the dithiothreitol depletion in [pmol.min^{-1}] as a function of $CuCl_2$ (b) and PQN (d) concentration in [nM]. (e) Green dots represent the ascorbic acid depletion, in [pmol.min^{-1}] as a function of PMs samples [µg.ml^{-1}] taken from a traffic site filter (Bern), and (f) orange dots represent the dithiothreitol depletion in [pmol.min^{-1}] as a function of PMs samples [µg.ml^{-1}] taken from an urban background winter filter (Grenoble). Dashed lines represent the modelled linear regressions. Each sample was analysed in triplicate, and the figures present average (dots), with the error bars representing ± 1σ.

https://doi.org/10.5194/egusphere-2025-2021
Preprint. Discussion started: 26 May 2025

As shown in Fig. 5(c), the AA response towards PQN over the [5 – 150] nM range seems null. This result is in accordance with Pietrogrande et al. (2022b), which demonstrated the sensitivity of OP^{AA} to PQN for concentrations above 1 µM (at $[AA]_0$ = 100 µM). It is therefore likely that [PQN] used here were too low for a response to be detected by *ROS-Online*. The relatively poor linearity observed in Fig. 5(b) is probably due to the low sensitivity of DTT to Cu(II). This result agrees well with what we observed during Exp. 1 and 2 at LOCIE bench (Fig. 4(b)). However, Fig. 5 (e) and (f) shows that the *ROS-Online* response is linear over the wide range of concentrations of PM extracts considered in this work i.e. from 0.05 to 1.86 µg PM.ml^{-1} corresponding to PM ambient concentrations between 5 to 180 µg.m^{-3}. The response is highly linear on both assays, with determination coefficient R^2 = 0.995 for AA (Bern sample) and R^2 = 0.990 for DTT (Grenoble sample).

Table 5. Figures of merit for the calibration experiments (standards solutions and PM samples)

Experiment / Assay	Pearson correlation coefficient - r	p-value	R^2	Blank	Intercept
[$CuCl_2$] ϵ [5– 50] nM / AA	0.986	4.30×10^{-5}	0.983	5.12 ± 1.14	8.09
[PQN] ϵ [5 – 150] nM / AA	-0.597	0.29	0.27	5.10 ± 0.68	5.72
PMs ϵ [0.05 – 1.05] µg.ml^{-1} / AA	0.997	1.96×10^{-4}	0.995	4.17± 0.22	4.59
[$CuCl_2$] ϵ [5– 50] nM / DTT	0.944	1.37×10^{-3}	0.962	36.61 ± 2.04	39.55
[PQN] ϵ [5 – 150] nM / DTT	0.993	7.30×10^{-4}	0.957	44.30 ± 1.07	50.71
PMs ϵ [0.05 – 1.86] µg.ml^{-1} / DTT	0.995	3.27×10^{-8}	0.990	39.24 ± 1.55	40.90

Table 5 reports the main characteristics of the linear regressions obtained with Cu(II) and PQN standard solutions and filter samples. Results are given without taking account the blank correction. As the intercept values are, to some extent, similar to the blank values, one can hypothesize that the non-zero intercept is likely related to the self-degradation of the antioxidants. This is supported by the fact that AA is sensitive to temperature and UV (Basak et al., 2023; Essodolom et al., 2020). In our protocol, the reacting solution containing AA is illuminated at 265 nm for 10 min in the FC and heated to 37°C, thus explaining the self-consumption of AA in the *ROS-Online* device. Similarly, both DTT and TNB are also sensitive to light (Damodaran, 1985; Eyer et al., 2003). In that case, the solution in the FC is illuminated at 412 nm for 15 min, resulting in the self-degradation of these reactants and finally to non-zero intercepts we observed for the DTT assay. The consideration of this issue subsequently led us to systematically perform a blank for each real atmospheric measurement. The difference in blank values observed for AA (4 to 5 pmol.min^{-1}) and for DTT (37 to 44 pmol.min^{-1}) assays may be due to the quality of the solutions used, particularly of the ultrapure water used either for the standards solutions or for the PM extracts. Additionally, the difference in blank values observed between both assays is probably due to the kinetics itself (reaction time, wavelength etc.).

https://doi.org/10.5194/egusphere-2025-2021
Preprint. Discussion started: 26 May 2025

5 Inter-comparison of online and offline measurements

This section describes an intercomparison study between *ROS-Online* and the offline methods implemented at IGE (Calas et al., 2019, Dominutti et al., 2024). The initial concentration of the reagents (AA, DTT, TNB) can significantly influence OP measurement (Lin and Yu, 2019), requiring us to adapt the concentrations of the offline method compared to the routine conditions to enable a comprehensive comparison of *ROS-Online* and offline OP techniques. Therefore, same samples and identical initial antioxidant quantity of matter, or moles' number n ($n_{AA_0} = 2.40 \times 10^{-9}$ mol ; $n_{DTT_0} = 1.25 \times 10^{-9}$ mol) were used in the respective measurement cells, i.e. flow cells or plate reader wells for online and offline methods, respectively. The calculation of absorbance has also been adjusted to these new conditions. For these experiments, the *ROS-Online* samples (control and PM samples) were introduced directly in the liquid form into the BioSampler® without pumping atmospheric air. The comparison between online and offline methods was made by analysing in triplicate the samples prepared and already described in Section 4. The three replicates used to calculate the standard deviations for the online method were performed within the same day. For the offline measurements, standard deviations were calculated using the 6 x 3 replicates =18 readings of the TECAN microplate reader.

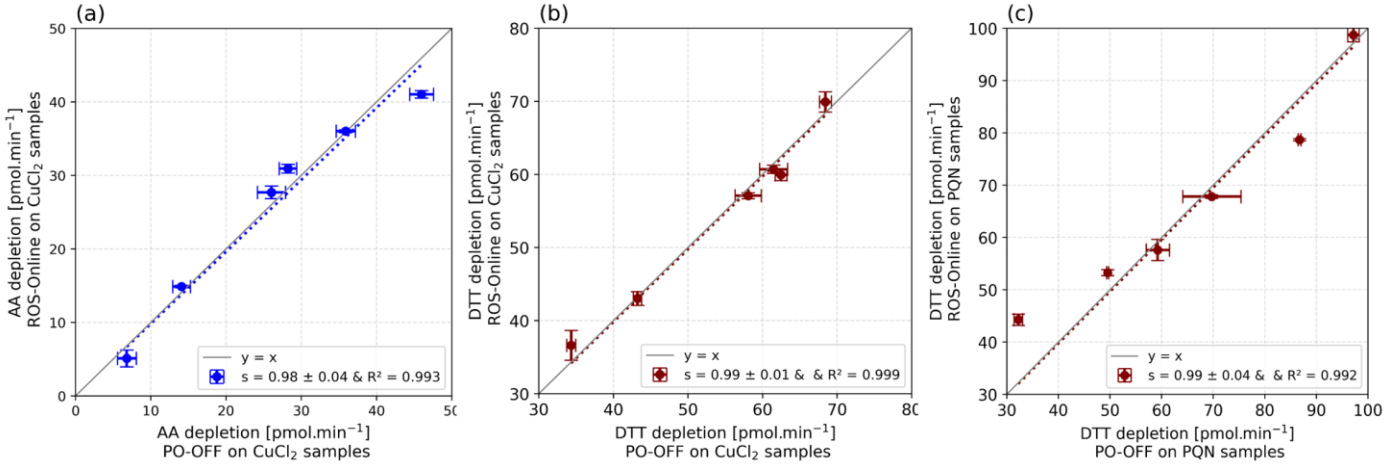

Figure 6. Comparison of offline and online methods using: (a) and (b) $CuCl_2$ samples for AA and DTT assays, respectively and (c) PQN samples on DTT assay. Each sample was analysed in triplicate, with both methods. The vertical error bar represents ± 1σ and the horizontal error bar represents the TECAN microplate variability of 18 measurements (6 readings for each triplicate of each range point). Grey lines represent the line y = x.

Fig. 6 (a)-(c) shows the results of the intercomparison (no blank correction) for the positive control solutions of $CuCl_2$ and PQN as analysed by *ROS-Online* and the offline IGE method. These plots demonstrated the excellent concordance between the 2 methods with linear regressions having $R^2 > 0.99$ and slopes (s) close to 1 ($s = 0.99$ for all three positive controls).

https://doi.org/10.5194/egusphere-2025-2021
Preprint. Discussion started: 26 May 2025

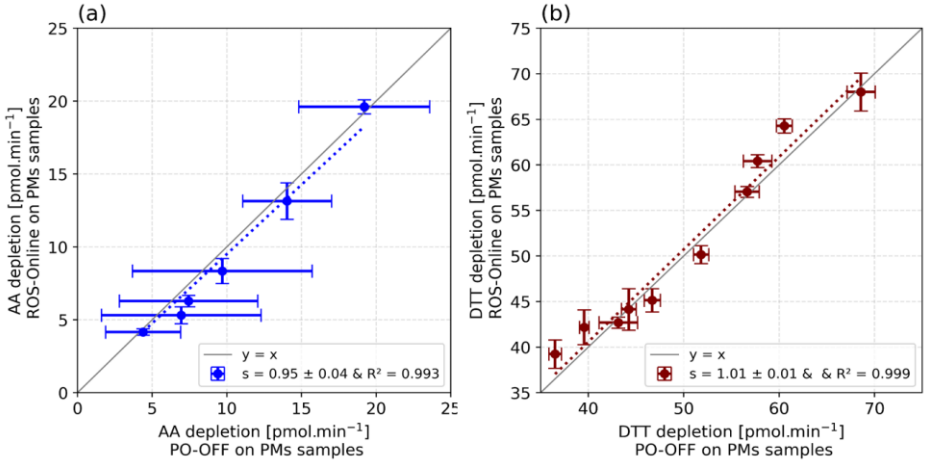

Figure 7. Comparison of offline and online methods using: (a) Bern traffic site filter for AA assay, and (b) Grenoble urban background winter filter for DTT assay. Each sample was analysed in triplicate with both methods. The vertical error bar represents ± 1σ and the horizontal error bar represents the TECAN microplate variability of 18 measurements (6 readings for each triplicate of each range point). Grey lines represent the line y = x.

Fig. 7 shows the results of *ROS-Online vs* offline analyses with AA and DTT assays when exposed to PM_{10} concentrations in the range [0.05 – 1.05] and [0.05 – 1.86] µg PM.ml^{-1} for AA and DTT assays, respectively. Quite large error bars on the TECAN microplate reader when measuring AA depletion can be noticed. However, even in that case, correlations coefficients of $R^2 > 0.99$ with *s* values close to 1 ($s = 0.95 \pm 0.04$ and $s = 1.01 \pm 0.01$, for AA and DTT assays, respectively) show again a very similar response between the two techniques with PM extracts. These results are encouraging in the way of providing measurements comparable to the offline methods, themselves currently under harmonisation and standardisation (Dominutti et al., 2024) to comply with response to the new European Directive on air quality.

6 Real-life case study: daily variation of OP^{AA} near a major roadway

6.1 Site sampling and meteorological conditions

The *ROS-Online* device was deployed from September 1st to September 15th 2023 at the air quality monitoring station « Les Bossons » from the air quality monitoring network in Auvergne – Rhône-Alpes. This site is located in the Arve Valley (45°54'26" N; 6°50'45; 1049 m a.s.l - https://www.atmo-auvergnerhonealpes.fr/dataviz/mesures-aux-stations). It is subjected to frequent pollution episodes, particularly in winter due to temperature inversions and intense domestic biomass burning (Quimbayo-Duarte et al., 2021; Weber et al., 2018). This traffic site is located on the roadside of the "Route blanche" with an average of 6,300 vehicles (with a large share of trucks) every day during the sampling campaign. The instruments were sheltered in an enclosed cabin with a controlled temperature set at T = 22 ± 4°C. The station houses a continuous ambient air monitor 1405-F TEOM™ for PM_{10} mass concentration measurements, and a NO_x analyser (model APNA-370, HORIBA). Additional atmospheric observations for PM_{10} mass concentration (ambient air monitor 1405-F TEOM™) and O_3 (ambient ozone monitor – model APOA-370 - HORIBA) were

https://doi.org/10.5194/egusphere-2025-2021
Preprint. Discussion started: 26 May 2025

also obtained from the air quality monitoring station "Chamonix" (45°55'21" N; 6°52'512; 1038 m a.s.l), located in Chamonix's city centre, about 2 km away. Meteorological data were obtained from the « Passy » station, located 13 km west on a lower part of the Arve Valley (https://www.infoclimat.fr/opendata/) and are presented in supplementary material (Fig. S3). A rainfall episode began during the night of 13 to 14 September and lasted until the end of the campaign (15/09).

6.2 *ROS-Online* measurements set-up

To maximise the PMs collection, the instrument was set for a sample duration of 30 minutes at a flowrate of 10.5 l.min^{-1}. A 20 µm filter was placed on the inlet line in order to protect the instrument from larger particles that might have clogged the BioSampler® or damaged the FCs. The prototype operated continuously without technical failure during the 15-days campaign. Due to a focus on the AA assay, more likely to react to a traffic source than the DTT assay, OP^{DTT} measurements were maintained from September 1st to September 6th only, allowing a higher resolution of OP^{AA} measurements after this date. Blanks for both assays were very stable: mean blank depletion value for the AA assay was ω_{AA_0} = (0.58 ± 0.24) pmol.min^{-1} (342 occurrences, 15 days) and let us calculate a LOD of (1.30 ± 0.24) pmol.min^{-1}. For the DTT assay, ω_{DTT_0} = (25.4 ± 4.0) pmol.min^{-1} (over 118 occurrences, 6 days) and LOD = (37.3 ± 4.0) pmol.min^{-1}. Finally, evaporation during sampling was evaluated to be (1.3 ± 0.1) ml with minimum and maximum values of 0.8 and 1.9 ml, respectively, mainly depending on the temperature difference between the outside and the shelter's thermostated temperature. The BioSampler® was filled with 20 ml of MQ water.

6.3 Results

The weather conditions during the campaign were very stable from 1st to 13th September, with anticyclonic conditions leading to similar daily cycles of temperature, wind and humidity (Fig. S3). Fig. 8 shows the average daily cycles of OP measurements, taking into account the full data series for OP^{AA} (1st to 13th) and the overall available dataset of OP^{DTT} (1st to 6th).

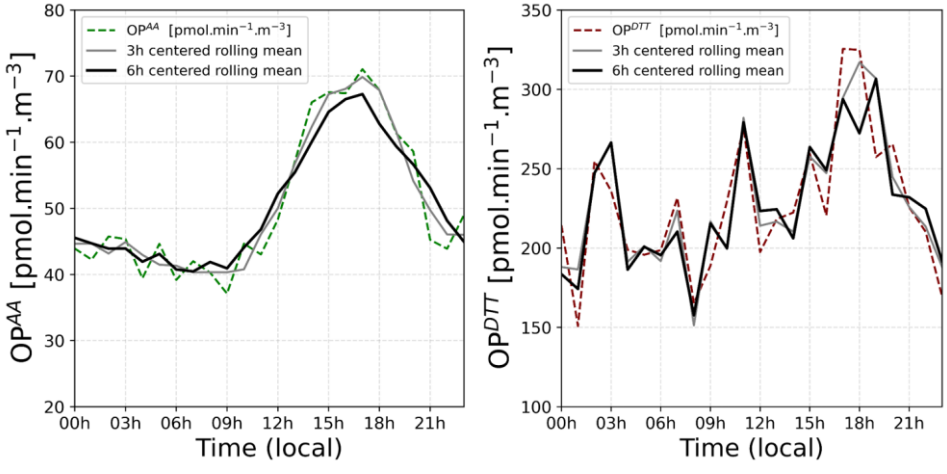

Figure 8. Average diurnal cycle of 13 days of OP^{AA} measurements (left) and of 6 days of OP^{DTT} measurements (right) observed at Les Bossons [pmol.min^{-1}.m^{-3}]. Dashed coloured lines show the averaged diurnal variation for all available measurements, grey and black lines the 3h and 6h rolling means.

https://doi.org/10.5194/egusphere-2025-2021
Preprint. Discussion started: 26 May 2025

Diurnal cycles of both OP^{AA} and OP^{DTT} measurements do not show the same variations, reflecting the different sensitivity to the aerosol composition of these two probes. OP^{AA} seems to stay at background level (40 pmol.min^{-1}.m^{-3}) at night and then rises up around 9 am until 4 pm, reaching twice its background value with a peak of ~ 70 pmol.min^{-1}.m^{-3}, before decreasing at a similar rate than its increase reaching background level again around midnight. The OP^{DTT} signal is less structured with OP values ~ 5 times that of OP^{AA} at background value (midnight). OP^{DTT} signal exhibits 3 main peaks at ~ 3 am, noon and ~ 6 pm, reaching ~ 300 pmol.min^{-1}.m^{-3} for the latter peak. The signal drops rapidly to its background level from 9 pm onwards.

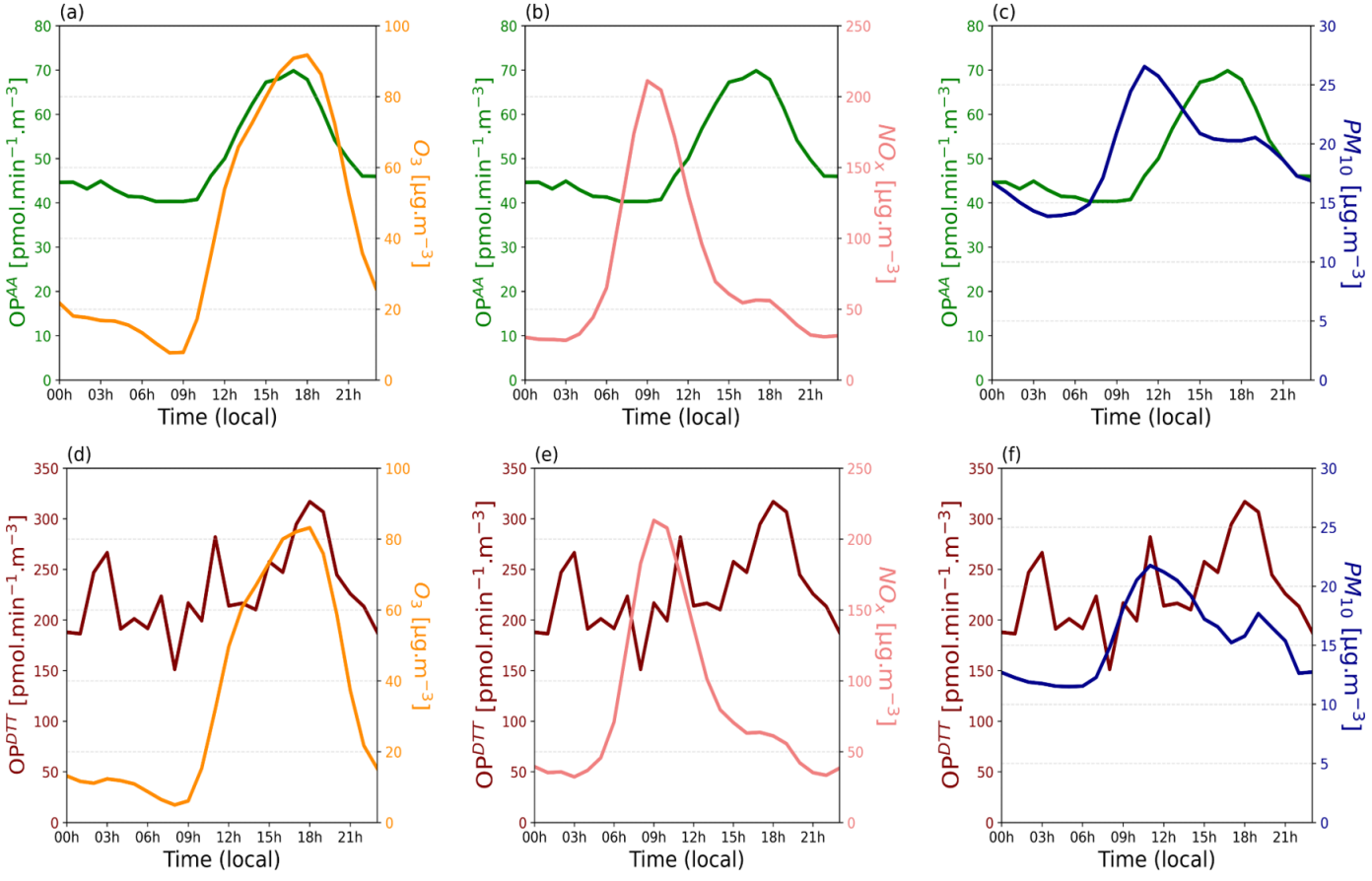

Figure 9. Diurnal O_3 [µg.m^{-3}] (a) and (d) observed at the measuring sites Chamonix; NO_x [µg.m^{-3}] (b) and (e), and PM_{10} [µg.m^{-3}] (c) and (f), observed at the measuring sites Les Bossons. Green lines on plot (a), (b), and (d) represents OP^{AA} [pmol.min^{-1}.m^{-3}] and brown lines on plots (d), (e), and (f) OP^{DTT} [pmol.min^{-1}.m^{-3}]. The 3h rolling mean datasets are used for each parameter.

As shown if Fig. 9 (a), (b), (d) and (e), NO_x and O_3 diurnal cycles show common behaviours for urban traffic sites with maximum levels of NO_x reached in the morning (Fig. 9 (b) and (e)) and maximum ozone concentration in late afternoon (Fig. 9 (a) and (d)), according to the well-established photochemical equilibrium relationship (Leighton, 1961). OP^{AA} signal is following the atmospheric photochemistry with a strong correlation with the evolution of the ozone concentration, both curves peaking in late afternoon (Fig 9 (a)). While our laboratory experiments showed that ozone had only a limited effect on the OP^{AA} (section 3.2.1.), this covariation is probably the result of the rising of PM concentrations in the afternoon (Fig. 9 (c)) due to primary but more likely

https://doi.org/10.5194/egusphere-2025-2021
Preprint. Discussion started: 26 May 2025

secondary emissions as well as boundary layer evolutions. Oxidation (aging) of PM in the afternoon, as shown with AMS measurement at a nearby site during the DECOMBIO project (Jaffrezo et al., 2018), may explain the delay between OP^{AA} and PM peaks on Fig. 9 (c).

The general behaviour of OP^{DTT} signal is similar to that of OP^{AA}, especially, OP^{DTT} higher peak corresponds to the O_3 peak (Fig. 9 (d)), which could again be explain by the oxidation of PM (Fig. 9 (f)). However, AA and DTT assays provide different information: the sharper OP^{DTT} signal, with 2 narrow peaks observed at around 3 am and 12 pm, may illustrate a local influence from sources or processes to be identified. Finally, during the rainy episode (13^{th} to 15^{th} of September) a resulting loss of PM_{10} and OP^{AA} diurnal cyclicity was observed, probably due to PM scavenging and / or perturbation of a change in boundary layer dynamics. Nevertheless, the OP^{AA} signal increased, still following the O_3 daily maximum levels during those 3 rainy days (see supplementary section 2.1). Overall, this short field study with the *ROS-Online* device shows that it is capable to perform dual time series of OP measurement with hourly measurements. These measurements indicate that OP can vary by nearly a factor of two within a day, due to a complex interplay between emissions, aging, and atmospheric dynamics.

7 Conclusions and perspectives

The *ROS-Online* device represents a significant leap forward in measuring the oxidative potential (OP) of ambient particulate matter and soluble gases. Its innovative design, incorporating dual independent lines for simultaneous OP^{AA} and OP^{DTT} assays, allows for near-real-time measurements with high reliability and specificity. Notably, its adaptability to collect both particulate and (soluble) gaseous pollutants provides a more comprehensive assessment of air quality compared to the traditional offline methods that collect PM only. The high linearity and low limits of detection (0.58 ± 0.24) $pmol.min^{-1}$ for AA and (25.4 ± 4.0) $pmol.min^{-1}$ for DTT, underscore its superior performance relative to existing prototypes. The *ROS-Online* device underwent controlled experiments and field tests to evaluate its performance and versatility.

The experiments in Section 3. provided insights into the oxidative potential (OP) responses of two assays, OP^{AA} and OP^{DTT}, when exposed to different aerosol compositions and concentrations. The OP^{AA} assay confirmed its strong sensitivity to metals, particularly $CuCl_2$, showing a proportional decrease in OP with decreasing PM concentration, while OP^{DTT} appeared to reach a saturation point, suggesting a possible reaction plateau. For naphthoquinone (NQ), OP values increased with PM concentration, though not proportionally, likely due to complex aerosol generation dynamics and surface interactions. These findings highlight the different reactivity mechanisms of the two assays towards inorganic and organic aerosols.

Calibration using $CuCl_2$ and 9,10-phenanthrenequinone (PQN) demonstrated good linearity for both OP^{AA} and OP^{DTT} assays, highlighting its sensitivity to both inorganic and organic classes of atmospheric oxidants. Intercomparison with established offline method confirmed efficiency, with high correlation coefficients ($R^2 > 0.90$) for both assays on a large range of concentrations, which is very encouraging for future deployment of *ROS-Online*. However, in order to associate offline and online measurements, thorough investigations need to be carried out to determine particle trapping between the two methods, exposure times, intrinsic OP values at different sites subjected to different atmospheres, etc.

https://doi.org/10.5194/egusphere-2025-2021
Preprint. Discussion started: 26 May 2025

Field deployment at an urban background site over a 15-day period provided continuous, near-real-time measurements of OP^{AA} and OP^{DTT}. The data revealed distinct diurnal patterns, with OP^{AA} peaking in the afternoon, correlating with photochemical activity and pollutant levels (O_3, and PM_{10}). OP^{DTT} measurements showed analogous, but not equivalent trends, with additional peaks indicating sensitivity to localized sources. The device's stability and consistent performance throughout the campaign underscore its suitability for long-term air quality monitoring.

A key strength of *ROS-Online* is its versatility across diverse environmental conditions. The possibility to adapt antioxidant concentrations allows OP measurements in both relatively clean European urban environments and highly polluted regions and or industrial sites, where particulate matter concentrations are significantly higher. This flexibility ensures accurate assessments regardless of pollution levels, making the device suitable for global deployment.

The device's ability to operate continuously to varying pollution levels reinforces its potential for integration into air quality networks worldwide. Its short temporal resolution (~ 1 hour) enables dynamic tracking of fast-changing atmospheric conditions, essential for understanding pollutant health impacts. Moreover, its sturdiness, demonstrated by continuous operation in field tests, highlights its potential for deployment in urban environments, industrial sites, and high-pollution areas.

ROS-Online's ability to interface with other online chemical analysers positions it as a valuable tool for source apportionment and health risk assessment, supporting regulatory efforts and advancing public health research. These innovations open new pathways for integrating OP measurements into routine air quality monitoring. The device not only meets the growing demand for precise, real-time air quality data but also aligns with the European directive on air quality, emphasizing the relevance of oxidative potential in health studies. Its deployment across air quality stations could be pivotal for pollution monitoring, paving the way for more targeted mitigation strategies and better public health status.

Data availability: The data are available upon request

Supplement: The supplement related to this article is available online at:

Author contributions: GU, and J-LJ funded the project. The *ROS-Online* instrument was designed and developed by GF, LR, LP and AB under the supervision of GU and J-LJ. LR, GF and LP developed the LabVIEW instrument control software, with the coordination of AB. JC, MB, TM and AM carried out laboratory tests and analyses for the calibration and intercomparison of online and offline methods under the supervision of AB and GU. AB and BG designed, established and carried out the tests in the vein. Finally, AB designed, established and carried out the ozone tests. AB, BG, SH, J-LJ and GU wrote the manuscript. All co-authors reviewed the manuscript.

Competing interests: The authors declare that they have no conflict of interest

https://doi.org/10.5194/egusphere-2025-2021
Preprint. Discussion started: 26 May 2025

Acknowledgements: The authors greatly thank the analytical staff of the IGE Air-O-Sol platform and the technical staff of the IGE for their help and support. Special thanks are due to S. Houdier, whose diligent work on the review process and meticulous English editing greatly enhanced the quality of this paper

Financial support: The research underpinning these results was supported by funding from UGA grants, including the Innovative Grant (2016) and Labex@2020 Valorisation (2017), as well as the CNRS Pre-Maturation Grant. Additionally, this work was partially funded by SATT Linksium.

References

BioSampler: https://www.skcltd.com/products2/bioaerosol-sampling/biosampler.html, last access: 9 July 2024.

State of Global Air Report 2024 | State of Global Air: https://www.stateofglobalair.org/resources/report/state-global-air-report-2024, last access: 16 December 2024.

Ayres, J. G., Borm, P., Cassee, F. R., Castranova, V., Donaldson, K., Ghio, A., Harrison, R. M., Hider, R., Kelly, F., Kooter, I. M., Marano, F., Maynard, R. L., Mudway, I., Nel, A., Sioutas, C., Smith, S., Baeza-Squiban, A., Cho, A., Duggan, S., and Froines, J.: Evaluating the Toxicity of Airborne Particulate Matter and Nanoparticles by Measuring Oxidative Stress Potential—A Workshop Report and Consensus Statement, Inhalation Toxicology, 20, 75–99, https://doi.org/10.1080/08958370701665517, 2008.

Basak, S., Shaik, L., and Chakraborty, S.: Effect of ultraviolet and pulsed light treatments on ascorbic acid content in fruit juices-A review of the degradation mechanism, Food Chemistry Advances, 2, 100333, https://doi.org/10.1016/j.focha.2023.100333, 2023.

Bates, J. T., Weber, R. J., Abrams, J., Verma, V., Fang, T., Klein, M., Strickland, M. J., Sarnat, S. E., Chang, H. H., Mulholland, J. A., Tolbert, P. E., and Russell, A. G.: Reactive Oxygen Species Generation Linked to Sources of Atmospheric Particulate Matter and Cardiorespiratory Effects, Environ. Sci. Technol., 49, 13605–13612, https://doi.org/10.1021/acs.est.5b02967, 2015.

Bates, J. T., Fang, T., Verma, V., Zeng, L., Weber, R. J., Tolbert, P. E., Abrams, J. Y., Sarnat, S. E., Klein, M., Mulholland, J. A., and Russell, A. G.: Review of Acellular Assays of Ambient Particulate Matter Oxidative Potential: Methods and Relationships with Composition, Sources, and Health Effects, Environ. Sci. Technol., 17, 2019.

Bellini, E. and De Tullio, M. C.: Ascorbic Acid and Ozone: Novel Perspectives to Explain an Elusive Relationship, Plants (Basel), 8, 122, https://doi.org/10.3390/plants8050122, 2019.

Bøifot, K. O., Skogan, G., and Dybwad, M.: Sampling efficiency and nucleic acid stability during long-term sampling with different bioaerosol samplers, Environ Monit Assess, 196, 577, https://doi.org/10.1007/s10661-024-12735-7, 2024.

Borlaza, L. J., Weber, S., Marsal, A., Uzu, G., Jacob, V., Besombes, J.-L., Chatain, M., Conil, S., and Jaffrezo, J.-L.: Nine-year trends of PM_{10} sources and oxidative potential in a rural background site in France, Atmospheric Chemistry and Physics, 22, 8701–8723, https://doi.org/10.5194/acp-22-8701-2022, 2022.

Bresgen, N. and Eckl, P. M.: Oxidative stress and the homeodynamics of iron metabolism, Biomolecules, 5, 808–847, https://doi.org/10.3390/biom5020808, 2015.

Calas, A., Uzu, G., Martins, J. M. F., Voisin, D., Spadini, L., Lacroix, T., and Jaffrezo, J.-L.: The importance of simulated lung fluid (SLF) extractions for a more relevant evaluation of the oxidative potential of particulate matter, Sci Rep, 7, 11617, https://doi.org/10.1038/s41598-017-11979-3, 2017.

Calas, A., Uzu, G., Kelly, F. J., Houdier, S., Martins, J. M. F., Thomas, F., Molton, F., Charron, A., Dunster, C., Oliete, A., Jacob, V., Besombes, J.-L., Chevrier, F., and Jaffrezo, J.-L.: Comparison between five acellular oxidative potential measurement assays performed with detailed chemistry on PM10 samples from the city of Chamonix (France), Atmos. Chem. Phys., 18, 7863–7875, https://doi.org/10.5194/acp-18-7863-2018, 2018a.

Calas, A., Uzu, G., Kelly, F. J., Houdier, S., Martins, J. M. F., Thomas, F., Molton, F., Charron, A., Dunster, C., Oliete, A., Jacob, V., Besombes, J.-L., Chevrier, F., and Jaffrezo, J.-L.: Comparison between five acellular oxidative potential measurement assays performed with detailed chemistry on PM10 samples from the city of Chamonix (France), Atmos. Chem. Phys., 18, 7863–7875, https://doi.org/10.5194/acp-18-7863-2018, 2018b.

Campbell, S. J., Utinger, B., Lienhard, D. M., Paulson, S. E., Shen, J., Griffiths, P. T., Stell, A. C., and Kalberer, M.: Development of a Physiologically Relevant Online Chemical Assay To Quantify Aerosol Oxidative Potential, Anal. Chem., 91, 13088–13095, https://doi.org/10.1021/acs.analchem.9b03282, 2019.

Campbell, S. J., Utinger, B., Barth, A., Paulson, S. E., and Kalberer, M.: Iron and Copper Alter the Oxidative Potential of Secondary Organic Aerosol: Insights from Online Measurements and Model Development, Environ. Sci. Technol., acs.est.3c01975, https://doi.org/10.1021/acs.est.3c01975, 2023.

Carlino, A., Romano, M. P., Lionetto, M. G., Contini, D., and Guascito, M. R.: An Overview of the Automated and On-Line Systems to Assess the Oxidative Potential of Particulate Matter, Atmosphere, 14, 256, https://doi.org/10.3390/atmos14020256, 2023.

Chang, Y.-P., Wu, S.-J., Lin, M.-S., Chiang, C.-Y., and Huang, G. G.: Ionic-strength and pH dependent reactivities of ascorbic acid toward ozone in aqueous micro-droplets studied by aerosol optical tweezers, Phys. Chem. Chem. Phys., 23, 10108–10117, https://doi.org/10.1039/D0CP06493A, 2021.

Charrier, J. G. and Anastasio, C.: On dithiothreitol (DTT) as a measure of oxidative potential for ambient particles: evidence for the importance of soluble transition metals, Atmos. Chem. Phys., 12, 9321–9333, https://doi.org/10.5194/acp-12-9321-2012, 2012.

Chen, L., Gonze, E., Ondarts, M., Outin, J., and Gonthier, Y.: Electrostatic precipitator for fine and ultrafine particle removal from indoor air environments, Separation and Purification Technology, 247, 116964, https://doi.org/10.1016/j.seppur.2020.116964, 2020.

Cho, A. K., Sioutas, C., Miguel, A. H., Kumagai, Y., Schmitz, D. A., Singh, M., Eiguren-Fernandez, A., and Froines, J. R.: Redox activity of airborne particulate matter at different sites in the Los Angeles Basin, Environmental Research, 99, 40–47, https://doi.org/10.1016/j.envres.2005.01.003, 2005.

Daellenbach, K. R., Uzu, G., Jiang, J., Cassagnes, L.-E., Leni, Z., Vlachou, A., Stefenelli, G., Canonaco, F., Weber, S., Segers, A., Kuenen, J. J. P., Schaap, M., Favez, O., Albinet, A., Aksoyoglu, S., Dommen, J., Baltensperger, U., Geiser, M., El Haddad, I., Jaffrezo, J.-L., and Prévôt, A. S. H.: Sources of particulate-matter air pollution and its oxidative potential in Europe, Nature, 587, 414–419, https://doi.org/10.1038/s41586-020-2902-8, 2020.

Damodaran, S.: Estimation of disulfide bonds using 2-nitro-5-thiosulfobenzoic acid: Limitations, Analytical Biochemistry, 145, 200–204, https://doi.org/10.1016/0003-2697(85)90348-3, 1985.

https://doi.org/10.5194/egusphere-2025-2021
Preprint. Discussion started: 26 May 2025

Delfino, R. J., Staimer, N., Tjoa, T., Gillen, D. L., Schauer, J. J., and Shafer, M. M.: Airway inflammation and oxidative potential of air pollutant particles in a pediatric asthma panel, J Expo Sci Environ Epidemiol, 23, 466–473, https://doi.org/10.1038/jes.2013.25, 2013.

Delgado-Saborit, J. M., Alam, M. S., Godri Pollitt, K. J., Stark, C., and Harrison, R. M.: Analysis of atmospheric concentrations of quinones and polycyclic aromatic hydrocarbons in vapour and particulate phases, Atmospheric Environment, 77, 974–982, https://doi.org/10.1016/j.atmosenv.2013.05.080, 2013.

Denier van der Gon, H., Gerlofs-Nijland, M., Gehrig, R., Gustafsson, M., Janssen, N., Harrison, R., Hulskotte, J., Johansson, C., Jozwicka, M., Keuken, M., Krijgsheld, K., Ntziachristos, L., Riediker, M., and Cassee, F.: The Policy Relevance of Wear Emissions from Road Transport, Now and in the FutureAn International Workshop Report and Consensus Statement, Journal of the Air & Waste Management Association (1995), 63, 136–49, https://doi.org/10.1080/10962247.2012.741055, 2013.

Dominutti, P. A., Borlaza, L. J. S., Sauvain, J.-J., Thuy, V. D. N., Houdier, S., Suarez, G., Jaffrezo, J.-L., Tobin, S., Trébuchon, C., Socquet, S., Moussu, E., Mary, G., and Uzu, G.: Source apportionment of oxidative potential depends on the choice of the assay: insights into 5 protocols comparison and implications for mitigation measures, Environ. Sci.: Atmos., 3, 1497–1512, https://doi.org/10.1039/D3EA00007A, 2023.

Dominutti, P. A., Jaffrezo, J.-L., Marsal, A., Mhadhbi, T., Elazzouzi, R., Rak, C., Cavalli, F., Putaud, J.-P., Bougiatioti, A., Mihalopoulos, N., Paraskevopoulou, D., Mudway, I. S., Nenes, A., Daellenbach, K. R., Banach, C., Campbell, S. J., Cigánková, H., Contini, D., Evans, G., Georgopoulou, M., Ghanem, M., Glencross, D. A., Guascito, M. R., Herrmann, H., Iram, S., Jovanović, M., Jovašević-Stojanović, M., Kalberer, M., Kooter, I. M., Paulson, S. E., Patel, A., Perdrix, E., Pietrogrande, M. C., Mikuška, P., Sauvain, J.-J., Seitanidi, A., Shahpoury, P., Souza, E. J. S., Steimer, S., Stevanovic, S., Suarez, G., Subramanian, P. S. G., Utinger, B., van Os, M. F., Verma, V., Wang, X., Weber, R. J., Yang, Y., Querol, X., Hoek, G., Harrison, R. M., and Uzu, G.: An interlaboratory comparison to quantify oxidative potential measurement in aerosol particles: challenges and recommendations for harmonisation, Atmospheric Measurement Techniques Discussions, 1–32, https://doi.org/10.5194/amt-2024-107, 2024.

Dominutti, P. A., Jaffrezo, J.-L., Marsal, A., Mhadhbi, T., Elazzouzi, R., Rak, C., Cavalli, F., Putaud, J.-P., Bougiatioti, A., Mihalopoulos, N., Paraskevopoulou, D., Mudway, I., Nenes, A., Daellenbach, K. R., Banach, C., Campbell, S. J., Cigánková, H., Contini, D., Evans, G., Georgopoulou, M., Ghanem, M., Glencross, D. A., Guascito, M. R., Herrmann, H., Iram, S., Jovanović, M., Jovašević-Stojanović, M., Kalberer, M., Kooter, I. M., Paulson, S. E., Patel, A., Perdrix, E., Pietrogrande, M. C., Mikuška, P., Sauvain, J.-J., Seitanidi, K., Shahpoury, P., Souza, E. J. d S., Steimer, S., Stevanovic, S., Suarez, G., Subramanian, P. S. G., Utinger, B., van Os, M. F., Verma, V., Wang, X., Weber, R. J., Yang, Y., Querol, X., Hoek, G., Harrison, R. M., and Uzu, G.: An interlaboratory comparison to quantify oxidative potential measurement in aerosol particles: challenges and recommendations for harmonisation, Atmospheric Measurement Techniques, 18, 177–195, https://doi.org/10.5194/amt-18-177-2025, 2025.

Dovrou, E., Lelieveld, S., Poeschl, U., and Berkemeier, T.: The Contribution of Reactive Gas-phase Pollutants to Oxidative Stress in the Human Lung, 2021, GH15A-0609, 2021a.

Dovrou, E., Lelieveld, S., Poeschl, U., and Berkemeier, T.: The Contribution of Reactive Gas-phase Pollutants to Oxidative Stress in the Human Lung, 2021, GH15A-0609, 2021b.

Eiguren-Fernandez, A., Miguel, A., Lu, R., Purvis, K., Grant, B., Mayo, P., Stefano, E., Cho, A., and Froines, J.: Atmospheric formation of 9,10-phenanthraquinone in the Los Angeles air basin, Atmospheric Environment, 42, 2312–2319, https://doi.org/10.1016/j.atmosenv.2007.12.029, 2008.

Essodolom, P., Ekpetsi Chantal, B., Mamatchi, M., and Kousanta, A.: Effect of temperature on the degradation on acid ascorbic acid (vitamin C) contained in infant supplement flours during the preparation of porridges, IJAR, 8, 116–121, https://doi.org/10.21474/IJAR01/10605, 2020.

https://doi.org/10.5194/egusphere-2025-2021
Preprint. Discussion started: 26 May 2025

Eyer, P., Worek, F., Kiderlen, D., Sinko, G., Stuglin, A., Simeon-Rudolf, V., and Reiner, E.: Molar absorption coefficients for the reduced Ellman reagent: reassessment, Anal Biochem, 312, 224–227, https://doi.org/10.1016/s0003-2697(02)00506-7, 2003.

Fang, Verma, V., Bates, J. T., Abrams, J., Klein, M., Strickland, M. J., Sarnat, S. E., Chang, H. H., Mulholland, J. A., Tolbert, P. E., Russell, A. G., and Weber, R. J.: Oxidative potential of ambient water-soluble PM2.5 in the southeastern United States: contrasts in sources and health associations between ascorbic acid (AA) and dithiothreitol (DTT) assays, Atmos. Chem. Phys., 15, 2016a.

Fang, Verma, V., Bates, J. T., Abrams, J., Klein, M., Strickland, M. J., Sarnat, S. E., Chang, H. H., Mulholland, J. A., Tolbert, P. E., Russell, A. G., and Weber, R. J.: Oxidative potential of ambient water-soluble PM2.5 in the southeastern United States: contrasts in sources and health associations between ascorbic acid (AA) and dithiothreitol (DTT) assays, Atmos. Chem. Phys., 15, 2016b.

Fang, T., Verma, V., Guo, H., King, L. E., Edgerton, E. S., and Weber, R. J.: A semi-automated system for quantifying the oxidative potential of ambient particles in aqueous extracts using the dithiothreitol (DTT) assay: results from the Southeastern Center for Air Pollution and Epidemiology (SCAPE), Atmos. Meas. Tech., 12, 2015a.

Fang, T., Verma, V., Guo, H., King, L. E., Edgerton, E. S., and Weber, R. J.: A semi-automated system for quantifying the oxidative potential of ambient particles in aqueous extracts using the dithiothreitol (DTT) assay: results from the Southeastern Center for Air Pollution and Epidemiology (SCAPE), Atmos. Meas. Tech., 12, 2015b.

Fuller, S. J., Wragg, F. P. H., Nutter, J., and Kalberer, M.: Comparison of on-line and off-line methods to quantify reactive oxygen species (ROS) in atmospheric aerosols, Atmospheric Environment, 92, 97–103, https://doi.org/10.1016/j.atmosenv.2014.04.006, 2014.

Gao, D., Fang, T., Verma, V., Zeng, L., and Weber, R. J.: A method for measuring total aerosol oxidative potential (OP) with the dithiothreitol (DTT) assay and comparisons between an urban and roadside site of water-soluble and total OP, Atmos. Meas. Tech., 10, 2821–2835, https://doi.org/10.5194/amt-10-2821-2017, 2017.

Godri, K. J., Harrison, R. M., Evans, T., Baker, T., Dunster, C., Mudway, I. S., and Kelly, F. J.: Increased Oxidative Burden Associated with Traffic Component of Ambient Particulate Matter at Roadside and Urban Background Schools Sites in London, PLoS ONE, 6, e21961, https://doi.org/10.1371/journal.pone.0021961, 2011.

Guo, J., Lv, M., Liu, Z., Qin, T., Qiu, H., zhang, L., Lu, J., Hu, L., Yang, W., and Zhou, D.: Comprehensive performance evaluation of six bioaerosol samplers based on an aerosol wind tunnel, Environment International, 183, 108402, https://doi.org/10.1016/j.envint.2023.108402, 2024.

Jaffrezo, J.-L., Besombes, J.-L., Marchand, N., Mocnik, G., Brulfert, G., Chevrier, F., Bertrand, A., Jezek, I., and Allard, J.: DEconvolution de la contribution de la COMbustion de la BIOmasse aux particules dans la vallée de l'Arve. Projet DECOMBIO, report, IGE, ADEME, 2018.

Jiang, Ahmed, Canchola, Chen, and Lin: Use of Dithiothreitol Assay to Evaluate the Oxidative Potential of Atmospheric Aerosols, Atmosphere, 10, 571, https://doi.org/10.3390/atmos10100571, 2019.

Jiang, H., Ahmed, C. M. S., Zhao, Z., Chen, J. Y., Zhang, H., Canchola, A., and Lin, Y.-H.: Role of functional groups in reaction kinetics of dithiothreitol with secondary organic aerosols, Environmental Pollution, 263, 114402, https://doi.org/10.1016/j.envpol.2020.114402, 2020.

Kachur, A. V., Held, K. D., Koch, C. J., and Biaglow, J. E.: Mechanism of Production of Hydroxyl Radicals in the Copper-Catalyzed Oxidation of Dithiothreitol, Radiation Research, 147, 409, https://doi.org/10.2307/3579496, 1997.

King, L. E. and Weber, R. J.: Development and testing of an online method to measure ambient fine particulate reactive oxygen species (ROS) based on the 2',7'-dichlorofluorescin (DCFH) assay, Atmos. Meas. Tech., 6, 1647–1658, https://doi.org/10.5194/amt-6-1647-2013, 2013.

Kumagai, Y., Koide, S., Taguchi, K., Endo, A., Nakai, Y., Yoshikawa, T., and Shimojo, N.: Oxidation of Proximal Protein Sulfhydryls by Phenanthraquinone, a Component of Diesel Exhaust Particles, Chem. Res. Toxicol., 15, 483–489, https://doi.org/10.1021/tx0100993, 2002.

Leighton, P.: Photochemistry of Air Pollution - 1st Edition, 1961.

Leni, Z., Cassagnes, L. E., Daellenbach, K. R., Haddad, I. E., Vlachou, A., Uzu, G., Prévôt, A. S. H., Jaffrezo, J.-L., Baumlin, N., Salathe, M., Baltensperger, U., Dommen, J., and Geiser, M.: Oxidative stress-induced inflammation in susceptible airways by anthropogenic aerosol, PLOS ONE, 15, e0233425, https://doi.org/10.1371/journal.pone.0233425, 2020.

Li, J., Leavey, A., Wang, Y., O'Neil, C., Wallace, M. A., Burnham, C.-A. D., Boon, A. C., Babcock, H., and Biswas, P.: Comparing the performance of 3 bioaerosol samplers for influenza virus, J Aerosol Sci, 115, 133–145, https://doi.org/10.1016/j.jaerosci.2017.08.007, 2018.

Li, Q., Wyatt, A., and Kamens, R. M.: Oxidant generation and toxicity enhancement of aged-diesel exhaust, Atmospheric Environment, 43, 1037–1042, https://doi.org/10.1016/j.atmosenv.2008.11.018, 2009.

Lin, H., Chen, Q., Wang, M., and Chang, T.: Oxidation potential and coupling effects of the fractionated components in airborne fine particulate matter, Environmental Research, 213, 113652, https://doi.org/10.1016/j.envres.2022.113652, 2022.

Lin, P. and Yu, J. Z.: Generation of Reactive Oxygen Species Mediated by Humic-like Substances in Atmospheric Aerosols, Environ. Sci. Technol., 45, 10362–10368, https://doi.org/10.1021/es2028229, 2011.

Lin, X.-T., Hsu, N.-Y., Wang, J.-R., Chen, N.-T., Su, H.-J., and Lin, M.-Y.: Development of an efficient viral aerosol collector for higher sampling flow rate, Environ Sci Pollut Res, 25, 3884–3893, https://doi.org/10.1007/s11356-017-0754-z, 2018.

Liu, X., Zhang, X., Wang, T., Jin, B., Wu, L., Lara, R., Monge, M., Reche, C., Jaffrezo, J.-L., Uzu, G., Dominutti, P., Darfeuil, S., Favez, O., Conil, S., Marchand, N., Castillo, S., de la Rosa, J. D., Stuart, G., Eleftheriadis, K., Diapouli, E., Gini, M. I., Nava, S., Alves, C., Wang, X., Xu, Y., Green, D. C., Beddows, D. C. S., Harrison, R. M., Alastuey, A., and Querol, X.: PM10-bound trace elements in pan-European urban atmosphere, Environmental Research, 260, 119630, https://doi.org/10.1016/j.envres.2024.119630, 2024.

Manigrasso, M., Costabile, F., Liberto, L. D., Gobbi, G. P., Gualtieri, M., Zanini, G., and Avino, P.: Size resolved aerosol respiratory doses in a Mediterranean urban area: From PM10 to ultrafine particles, Environment International, 141, 105714, https://doi.org/10.1016/j.envint.2020.105714, 2020.

Manisalidis, I., Stavropoulou, E., Stavropoulos, A., and Bezirtzoglou, E.: Environmental and Health Impacts of Air Pollution: A Review, Frontiers in Public Health, 8, 2020.

Mescioglu, E., Paytan, A., Mitchell, B. W., and Griffin, D. W.: Efficiency of bioaerosol samplers: a comparison study, Aerobiologia, 37, 447–459, https://doi.org/10.1007/s10453-020-09686-0, 2021.

Møller, P., Danielsen, P. H., Karottki, D. G., Jantzen, K., Roursgaard, M., Klingberg, H., Jensen, D. M., Christophersen, D. V., Hemmingsen, J. G., Cao, Y., and Loft, S.: Oxidative stress and inflammation generated DNA damage by exposure to air pollution particles, Mutat Res Rev Mutat Res, 762, 133–166, https://doi.org/10.1016/j.mrrev.2014.09.001, 2014.

https://doi.org/10.5194/egusphere-2025-2021
Preprint. Discussion started: 26 May 2025

Møller, P., Scholten, R., Roursgaard, M., and Krais, A.: Inflammation, oxidative stress and genotoxicity responses to biodiesel emissions in cultured mammalian cells and animals, Critical Reviews in Toxicology, 50, 1–19, https://doi.org/10.1080/10408444.2020.1762541, 2020.

Mudway, I. S., Stenfors, N., Duggan, S. T., Roxborough, H., Zielinski, H., Marklund, S. L., Blomberg, A., Frew, A. J., Sandström, T., and Kelly, F. J.: An in vitro and in vivo investigation of the effects of diesel exhaust on human airway lining fluid antioxidants, Archives of Biochemistry and Biophysics, 423, 200–212, https://doi.org/10.1016/j.abb.2003.12.018, 2004.

Park, M., Joo, H. S., Lee, K., Jang, M., Kim, S. D., Kim, I., Borlaza, L. J. S., Lim, H., Shin, H., Chung, K. H., Choi, Y.-H., Park, S. G., Bae, M.-S., Lee, J., Song, H., and Park, K.: Differential toxicities of fine particulate matters from various sources, Sci Rep, 8, 17007, https://doi.org/10.1038/s41598-018-35398-0, 2018.

Perrone, M. R., Bertoli, I., Romano, S., Russo, M., Rispoli, G., and Pietrogrande, M. C.: PM2.5 and PM10 oxidative potential at a Central Mediterranean Site: Contrasts between dithiothreitol- and ascorbic acid-measured values in relation with particle size and chemical composition, Atmospheric Environment, 210, 143–155, https://doi.org/10.1016/j.atmosenv.2019.04.047, 2019.

Pietrogrande, M. C., Romanato, L., and Russo, M.: Synergistic and Antagonistic Effects of Aerosol Components on Its Oxidative Potential as Predictor of Particle Toxicity, Toxics, 10, 196, https://doi.org/10.3390/toxics10040196, 2022a.

Pietrogrande, M. C., Romanato, L., and Russo, M.: Synergistic and Antagonistic Effects of Aerosol Components on Its Oxidative Potential as Predictor of Particle Toxicity, Toxics, 10, 196, https://doi.org/10.3390/toxics10040196, 2022b.

Qu, J., Li, Y., Zhong, W., Gao, P., and Hu, C.: Recent developments in the role of reactive oxygen species in allergic asthma, J Thorac Dis, 9, E32–E43, https://doi.org/10.21037/jtd.2017.01.05, 2017.

Quimbayo-Duarte, J., Chemel, C., Staquet, C., Troude, F., and Arduini, G.: Drivers of severe air pollution events in a deep valley during wintertime: A case study from the Arve river valley, France, Atmospheric Environment, 247, 118030, https://doi.org/10.1016/j.atmosenv.2020.118030, 2021.

Rao, L., Zhang, L., Wang, X., Xie, T., Zhou, S., Lu, S., Liu, X., Lu, H., Xiao, K., Wang, W., and Wang, Q.: Oxidative Potential Induced by Ambient Particulate Matters with Acellular Assays: A Review, 21, 2020a.

Rao, L., Zhang, L., Wang, X., Xie, T., Zhou, S., Lu, S., Liu, X., Lu, H., Xiao, K., Wang, W., and Wang, Q.: Oxidative Potential Induced by Ambient Particulate Matters with Acellular Assays: A Review, 21, 2020b.

Sherif, E. M. and Park, S.-M.: Effects of 1,4-naphthoquinone on aluminum corrosion in 0.50 M sodium chloride solutions, Electrochimica Acta, 51, 1313–1321, https://doi.org/10.1016/j.electacta.2005.06.018, 2006.

Song, M., Oh, S.-H., Park, C., and Bae, M.-S.: Review: Analytical Procedure for Dithiothreitol-based Oxidative Potential of PM2.5, Asian Journal of Atmospheric Environment, 15, 13, 2021.

Stevanovic, S.: Oxidative potential of gas phase combustion emissions - An underestimated and potentially harmful component of air pollution from combustion processes, Atmospheric Environment, 2017.

Strak, M., Janssen, N. A. H., Godri, K. J., Gosens, I., Mudway, I. S., Cassee, F. R., Lebret, E., Kelly, F. J., Harrison, R. M., Brunekreef, B., Steenhof, M., and Hoek, G.: Respiratory Health Effects of Airborne Particulate Matter: The Role of Particle Size, Composition, and Oxidative Potential—The RAPTES Project, Environmental Health Perspectives, 120, 1183–1189, https://doi.org/10.1289/ehp.1104389, 2012.

https://doi.org/10.5194/egusphere-2025-2021
Preprint. Discussion started: 26 May 2025

Su, W.-C. and Vincent, J. H.: Towards a general semi-empirical model for the aspiration efficiencies of aerosol samplers in perfectly calm air, Journal of Aerosol Science, 35, 1119–1134, https://doi.org/10.1016/j.jaerosci.2004.04.003, 2004.

Turner, M. C., Andersen, Z. J., Baccarelli, A., Diver, W. R., Gapstur, S. M., Pope III, C. A., Prada, D., Samet, J., Thurston, G., and Cohen, A.: Outdoor air pollution and cancer: An overview of the current evidence and public health recommendations, CA: A Cancer Journal for Clinicians, 70, 460–479, https://doi.org/10.3322/caac.21632, 2020.

Utinger, B., Campbell, S. J., Bukowiecki, N., Barth, A., Gfeller, B., Freshwater, R., Ruegg, H.-R., and Kalberer, M.: An Automated Online Field Instrument to Quantify the Oxidative Potential of Aerosol Particles via Ascorbic Acid Oxidation, Aerosols/Laboratory Measurement/Instruments and Platforms, https://doi.org/10.5194/amt-2023-14, 2023.

Uzu, G., Sauvain, J.-J., Baeza-Squiban, A., Riediker, M., Sánchez Sandoval Hohl, M., Val, S., Tack, K., Denys, S., Pradère, P., and Dumat, C.: In vitro Assessment of the Pulmonary Toxicity and Gastric Availability of Lead-Rich Particles from a Lead Recycling Plant, Environ. Sci. Technol., 45, 7888–7895, https://doi.org/10.1021/es200374c, 2011.

Walker, M. D., Vincent, J. C., Benson, L., Stone, C. A., Harris, G., Ambler, R. E., Watts, P., Slatter, T., López-García, M., King, M.-F., Noakes, C. J., and Thomas, R. J.: Effect of Relative Humidity on Transfer of Aerosol-Deposited Artificial and Human Saliva from Surfaces to Artificial Finger-Pads, Viruses, 14, 1048, https://doi.org/10.3390/v14051048, 2022.

Weber, S., Uzu, G., Calas, A., Chevrier, F., Besombes, J.-L., Charron, A., Salameh, D., Ježek, I., Močnik, G., and Jaffrezo, J.-L.: An apportionment method for the oxidative potential of atmospheric particulate matter sources: application to a one-year study in Chamonix, France, Atmos. Chem. Phys., 18, 9617–9629, https://doi.org/10.5194/acp-18-9617-2018, 2018.

Weber, S., Uzu, G., Favez, O., Borlaza, L. J. S., Calas, A., Salameh, D., Chevrier, F., Allard, J., Besombes, J.-L., Albinet, A., Pontet, S., Mesbah, B., Gille, G., Zhang, S., Pallares, C., Leoz-Garziandia, E., and Jaffrezo, J.-L.: Source apportionment of atmospheric PM10; oxidative potential: synthesis of 15 year-round urban datasets in France, Atmos. Chem. Phys., 21, 11353–11378, https://doi.org/10.5194/acp-21-11353-2021, 2021.

WHO: https://www.who.int/news-room/fact-sheets/detail/ambient-(outdoor)-air-quality-and-health, last access: 29 May 2023.

Wittmaack, K.: In Search of the Most Relevant Parameter for Quantifying Lung Inflammatory Response to Nanoparticle Exposure: Particle Number, Surface Area, or What?, Environmental Health Perspectives, 115, 187–194, https://doi.org/10.1289/ehp.9254, 2007.

Wragg, F. P. H., Fuller, S. J., Freshwater, R., Green, D. C., Kelly, F. J., and Kalberer, M.: An automated online instrument to quantify aerosol-bound reactive oxygenspecies (ROS) for ambient measurement and health-relevant aerosol studies, Atmos. Meas. Tech., 9, 4891–4900, https://doi.org/10.5194/amt-9-4891-2016, 2016.

Yang, A., Jedynska, A., Hellack, B., Kooter, I., Hoek, G., Brunekreef, B., Kuhlbusch, T. A. J., Cassee, F. R., and Janssen, N. A. H.: Measurement of the oxidative potential of PM2.5 and its constituents: The effect of extraction solvent and filter type, Atmospheric Environment, 83, 35–42, https://doi.org/10.1016/j.atmosenv.2013.10.049, 2014.

Yang, M., Ahmed, H., Wu, W., Jiang, B., and Jia, Z.: Cytotoxicity of Air Pollutant 9,10-Phenanthrenequinone: Role of Reactive Oxygen Species and Redox Signaling, BioMed Research International, 2018, 1–15, https://doi.org/10.1155/2018/9523968, 2018.

Yu, H., Puthussery, J. V., and Verma, V.: A semi-automated multi-endpoint reactive oxygen species activity analyzer (SAMERA) for measuring the oxidative potential of ambient PM $_{2.5}$ aqueous extracts, Aerosol Science and Technology, 54, 304–320, https://doi.org/10.1080/02786826.2019.1693492, 2020a.

https://doi.org/10.5194/egusphere-2025-2021
Preprint. Discussion started: 26 May 2025

Yu, H., Puthussery, J. V., and Verma, V.: A semi-automated multi-endpoint reactive oxygen species activity analyzer (SAMERA) for measuring the oxidative potential of ambient PM $_{2.5}$ aqueous extracts, Aerosol Science and Technology, 54, 304–320, https://doi.org/10.1080/02786826.2019.1693492, 2020b.